Electrons and positrons in dense gases

A. G. Khrapak and I. T. Yakubov

Institute of High Temperatures, USSR Academy of Sciences
Usp. Fiz. Nauk **129**, 45–86 (September 1979)

The appearance of electrons or positrons in dense gaseous media produces a whole series of striking phenomena governed by the properties of the states of the light particles in the dense medium. The present review considers these phenomena systematically. The results of measurements of electron mobility and positron annihilation rates in moderately dense gases are discussed. Effects that arise as the density of the gas increases are considered. Self-trapped states become possible at high densities: these are bound states of the light particles with the medium, "clusters," "bubbles," or mixed-type formations. The fluctuon theory of these states is set forth, along with the results of experiments in which the light particles make transitions to new states. The possible existence of "orientation clusters" in gases consisting of polar molecules is investigated. Certain applications of the results to the theory of discharges in dense gases and liquids and to the theory of the weakly ionized nonideal plasma are discussed.

PACS numbers: 51.50. + v, 51.10. + y

CONTENTS

INTRODUCTION

The present review is devoted to phenomena that arise when light charged particles—electrons and positrons—appear in dense gases. The state of these particles in the gas changes radically as the density of the gas rises. This evidenced by observations of a sharp drop in electron mobility with increasing gas density, an exponential increase in the annihilation rate of slow positrons, and other experiments.

Qualitative effects can be observed even at moderately high densities and pressures (pressures in the tens of atmospheres at standard temperature). The reduced mobility μ/μ_0 increases with density in some gases and decreases in others. This decrease anticipates the striking phenomena caused by the formation of states in which electrons, positrons, or positronium atoms are bound to the medium. Clusters, orientation clusters, bubbles, or mixed-type formations may result, depending on the nature of the interaction.

The review considers conditions under which the electron (positron) density is so small that the inter-

 0038-5670/79/090703-24$01.10

action between these particles can be neglected. All of the principal effects are governed by the interaction between the light charged particle and atoms of the gas owing to the long wavelength of the light particle or the large charge/neutral interaction radius. Chapter 1 discusses the range of moderate densities (10^{20}–10^{21} cm^{-3}), in which it is sufficient to apply only the first density corrections. Chapter 2 discusses localization or trapping effects that arise at high densities (10^{21}–10^{22} cm^{-3}), when the interatomic interaction also becomes appreciable. Chapter 3 discusses some applications.

While the state of electrons and positrons in rarefied gases is comparatively well understood,[1-3] interest in dense gases has really come alive only in the last decade. Although completely different properties have been studied (for example, electron mobility and positron annihilation rate), the observed anomalies are governed by related phenomena. One of the objectives of the present review is to discuss effects that are common to all light particles in dense gases.

Dense gases represent the simplest case of the dense disordered medium. The problem of the electron in a dense environment of disordered scatterers[4-6] simulates a whole series of phenomena in various areas of physics, such as the physics of nonpolar liquids,[7] strongly doped semiconductors,[8,9] solutions of electrolytes,[7] and the nonideal plasma.[10] Theoretical study of the properties of electrons and positrons in dense gases relies in many respects on methods that are widely used in the theory of condensed disordered systems and were developed in Refs. 5, 11, 12.

1. ELECTRON MOBILITY IN MODERATELY DENSE GASES

Nonlinear effects due to the interaction of electrons (positrons) with the atoms (molecules) of a gas arise at densities such that the gas itself can be regarded as near-ideal. Their appearance results either from a large value of the electron wavelength or from a large effective radius of the electron-atom interaction potential. Therefore the most interesting effects should be expected in cold gases and in gases whose atoms possess high polarizability. Features of the interaction of the electrons with the gas atoms and molecules are most fully in evidence in such cases.

Density effects have been observed at densities $N = 10^{20}$–10^{21} cm^{-3} in studies of the mobility of electrons injected into a gas. Even at these not particularly high densities, the electron-atom interaction cannot be reduced to a series of successive pair-scattering events. As a result the electron mobility is not equal to the value μ_0 defined by the Lorentz formula

$$\mu_0 = \frac{e}{m\nu}, \quad \nu = Nqv; \tag{1.1}$$

where ν is the average frequency of collisions of the electron with atoms, q is the scattering cross section, v is the velocity of the electron, $v = \sqrt{2\varepsilon/m}$, and ε is its energy.

A qualitative effect has been observed in experiments of recent years. In most gases, for example in He and H_2, the reduced mobility μ/μ_0 decreases with increasing N. But μ/μ_0 increases in Ar and CH_4. This behavior of μ/μ_0 has been explained only recently in its relation to aspects of the interaction of electrons with atoms of gases of these groups.

Similarly, density effects should influence the state of the positron (and positronium) in dense gases. In the next section of this chapter we shall discuss measurements of positron annihilation rates in gases.

a) Mobility of thermalized electrons

Most of the measurements have been made by the direct "time-of-flight" method.[13] The quantity measured is the time for electrons that have been injected into the gas to drift between two electrodes. Since the distance between the electrodes is known, what is actually measured is the drift velocity W, $W = \mu F$, where F is the electric strength. Figure 1 shows results of measurements in He, H_2,[14,15] Ar,[16] and CH_4[17] in weak fields, i.e., under conditions such that the electrons are thermalized. Let us discuss the causes of the differing behavior of $W/W_0(N)$ in these gases.

Since the electron density is low, the electrons interact only with atoms of the gas. At moderate gas densities the interatomic interaction can be neglected. Therefore the electron is in a field $u(\mathbf{r})$ of randomly distributed scatterers,

$$u(\mathbf{r}) = \sum_j V(\mathbf{r} - \mathbf{R}_j), \tag{1.2}$$

where $V(\mathbf{r})$ is the potential of the electron-atom interaction and $\mathbf{R}_j$ is the coordinate of the jth atom. For slow electrons, $V(\mathbf{r})$ is determined by the scattering length L and the polarizability α of the atom.[18a] Let us first consider the case in which the polarizability is small.

If the fields of neighboring atoms do not overlap, $N|L|^3 \ll 1$, $V(\mathbf{r})$ can be represented in the form of a Fermi pseudopotential:

$$V(\mathbf{r}) = \frac{2\pi\hbar^2 L}{m}\delta(\mathbf{r}). \tag{1.3}$$

At low densities, the electron collides with atoms at a frequency $\nu = Nqv$, where $q = 4\pi L^2$ is the scattering cross section. When the electron wavelength $\lambda = \hbar/\sqrt{2m\varepsilon}$ becomes comparable to the path length $(qN)^{-1}$, successive scattering events are no longer independent. The effective collision frequency increases by the

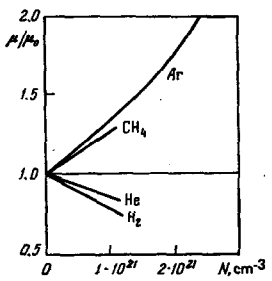

FIG. 1. Reduced drift velocity of thermalized electrons vs. density in various gases ($T = 300$ K).

interference correction:

$$\nu_{eff} = \nu (1 + \lambda q N). \tag{1.4}$$

This effect is the first density effect.[19]

The interference effect lowers the drift velocity,

$$\frac{W}{W_0} = 1 - \sqrt{\pi}\lambda_\beta q N, \tag{1.5}$$

where $\lambda_\beta = \hbar/\sqrt{2mT}$ is the thermal wavelength. For the He atom $L = 1.2a_0$, and for the H_2 molecule $L = 1.6a_0$. At $T = 300$ K and $N = 10^{21}$ cm^{-3} we obtain $W/W_0 - 1 \approx 0.1$, which agrees with the value observed in experiments (Fig. 1).

If the cross section $q(\varepsilon)$ depends very weakly on energy, relation (1.5) can be rewritten $W/W_0 = 1 - \eta N T^{-1/2}$, where η is a constant for a given gas. Schwartz[18b] analyzed the results of measurements in helium: η was indeed found to be constant upon variation of the temperature and density. The temperature was varied in a broad range, from 4.2 to 300 K.

Let us now consider the situation in a gas of high polarizability α. In this case the potential $V(\mathbf{r})$ cannot be regarded as short-range (1.3). The long-range polarization component of the potential $V(\mathbf{r}) = -\alpha e^2/2r^4$ is significant for scattering. Let us represent $V(\mathbf{r})$ as the sum of the short-range component (of electrostatic and exchange origin) and the polarization component:

$$V(\mathbf{r}) = \frac{2\pi\hbar^2 L}{m}\delta(\mathbf{r}) + \frac{\alpha e^2\pi^2}{2r_0}\delta(\mathbf{r}) - \frac{\alpha e^2}{2(r_0^3 + r^3)^2}. \tag{1.6}$$

The "atomic radius" r_0 is obviously of the order of the Bohr radius a_0. The potential (1.6) is applicable to slow electrons with long wavelengths $\lambda, \lambda \gg |L|, \lambda \gg r_0, \lambda^2 \gg \alpha a_0^{-1}$. The amplitude of scattering through an angle θ on the potential (1.6) has the form

$$f = L\left(1 + \frac{\pi\alpha}{2La_0\lambda}\sin\frac{\theta}{2}\right).$$

This theory agrees well with the results of measurements in rarefied gases.

The fact that the electron as it induces dipole moments on the atoms also induces a dipole-dipole interaction between them becomes important in dense gases. Dipoles oriented to the electron repel one another, lowering the resultant dipole moment of the atom. As a result, a multiplier that depends on density appears in the asymptotic form of the potential $V(r)$[20]:

$$V(r) = -\frac{\alpha e^2}{2r^4}\left(1 + \frac{8\pi}{3}\alpha N\right)^{-1}.$$

This multiplier is the permittivity of the gas. Thus, the electron-atom interaction in the medium is described by the potential

$$V(r) = \frac{2\pi\hbar^2 L}{m}\delta(r) + \frac{\alpha e^2\pi^2}{2r_0}\delta(r) - \frac{\alpha e^2}{2(r_0^3 + r^3)^2}\left(1 + \frac{8\pi}{3}\alpha N\right)^{-1}, \tag{1.7}$$

which can be applied for both moderate and high densities.[21] The latter will be done later, in Section d). At moderate densities, when $8\pi\alpha N/3 \ll 1$, the amplitude of scattering on $V(r)$ (1.7) takes the form

$$f(N) = L\left(1 + \frac{\pi\alpha}{2La_0\lambda}\sin\frac{\theta}{2}\right) + \frac{8\pi}{3}\alpha N \cdot \frac{\pi\alpha}{4a_0 r_0}. \tag{1.8}$$

The last term in (1.8) gives a positive density correction. If $L < 0$, f decreases with increasing N, and therefore W/W_0 increases.

This is precisely the situation in Ar and CH_4. For argon $L = -1.2a_0$, $\alpha = 11.1a_0^3$, and $r_0 = 1.2a_0$ (this value of r_0 was proposed in Ref. 22). At $T = 300$ K and $N = 10^{21}$ cm^{-3} we obtain an approximately 30% decrease in the effective cross section, which would explain the observed increase in W/W_0 (Fig. 1).[21] What is essential is that the effect need not be small. The small parameter is not the correction to the scattering amplitude, but the quantity $8\pi\alpha N/3$.

Mobilities in He and H_2 have been measured[23-27] at lower temperatures, 20–160 K, and densities up to $6 \cdot 10^{21}$ cm^{-3}. Figure 2 presents results obtained in Ref. 26. We observe first of all that the mobility decreases comparatively sharply with increasing N (not in inverse proportion to the density, $\sim N^{-1}$, but rather as $N^{-3/2}$ or N^{-2}). Secondly, μ does not depend on the temperature of the gas.[1)] This enables us to propose the following interpretation. In a dense cold medium, the electron has a "zero" energy $2\pi\hbar^2 LN/m$, which determines the velocity of its translational motion (in accordance, for example, with the Wigner-Seitz model[28] [see also Chap. 2, Sec. b)]. Therefore as long as $2\pi\hbar^2 LN/m \gg T$, we have the first-approximation mobility $\mu = (e/\hbar)(4\pi LN)^{-3/2}L^{-1}$. There are corrections to this quantity in the parameter $LN^{1/3}$, in much the same way as in the problem of the state of the positronium atom in matter.[29,30] This enables us to interpret the results shown in Fig. 2, although a properly conditioned description has not yet been obtained.

A low-mobility branch was observed[24] in addition to the relationship discussed above. Differences have arisen as to its treatment.[24,26,31] Bartels showed that this branch is related to the presence of impurity ions, chiefly O_2^-, in the gas.

b) Drift velocity of hot electrons

Interesting experimental data have been obtained in heating electric fields in which the average electron velocity exceeds the gas temperature T. In dense

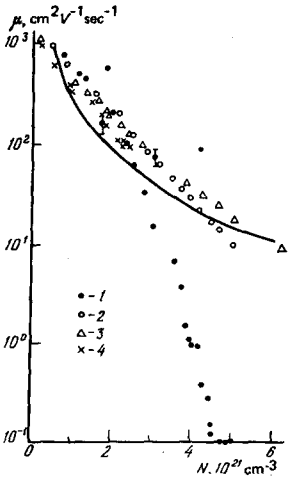

FIG. 2. Electron mobility μ as function of helium density[26] at various temperatures: $T(K) = 20.3$ (1), 52.8 (2), 77.3 (3) and 160 (4).

[1)] This does not mean that the electrons have made the transition to the trapped state. At 77 K this transition occurs at $N = 7 \cdot 10^{21}$ cm^{-3} [see Chap. 2, Sec. a]. In the experiment of Ref. 26, the transition occurred only at $T = 20.3$ K (see Fig. 2).

gases, the drift velocity W ceases to be a function of F/N alone. There is also a density dependence $W(F/N, N)$, which has been observed in a number of studies; see the review in Ref. 32.

Figure 3a shows values of W/W_0 plotted against F/N for various densities in hydrogen and argon. They were obtained by the time-of-flight method.[14,16] In both cases the largest deviations from unity are observed in low fields, when the electrons are thermalized. As a result of heating of the electrons, W/W_0 tends to unity. It is quickly understood from general considerations that any effects due to nonideality should vanish at high energies. However, more complex $W(F/N, N)$ relationships are observed in addition to the simple monotonic ones. Figure 3b shows plots obtained in methane[17] and ethane.[33] We shall put off discussion of the latter case until the next section; as for the nonmonotonic W/W_0 relation in CH_4, it results from the simultaneous appearance of the effects observed in Ar and H_2.[34]

In the single-electron approximation, the drift velocity can always be expressed in terms of the effective frequency ν_{eff}, $W = eF/m\nu_{\text{eff}}$. If we assume that the interaction does not affect the electron dispersion law, averaging of $\nu_{\text{eff}}(\varepsilon)$ over the energies ε takes place as usual[35]:

$$W = -\frac{2}{3}\frac{eF}{m}\int_0^\infty \frac{\varepsilon^{3/2}\,d\varepsilon}{\nu_{\text{eff}}(\varepsilon)}\frac{\partial f}{\partial \varepsilon}. \tag{1.9}$$

We have for the electron distribution function[35]

$$f(\varepsilon) = f(0)\exp\left[-\int_0^\varepsilon \left(T + \frac{2e^2F^2}{3\delta m\nu_{\text{eff}}}\right)^{-1} d\varepsilon\right], \tag{1.10}$$

where δ is the fraction of the energy lost in the collision, $\delta = 2m/M$ for small F/N. In strong fields, δ increases as a result of inelastic processes.[35]

In a gas with low polarizability, when $q(\varepsilon)$ does not depend on ε, we take the interference effect (1.4) into account. W/W_0 agrees with (1.5) for thermalized electrons. For very hot electrons, when $T \ll 2e^2F^2(3m\nu^2)^{-1}$, we obtain with (1.10) and (1.9)

$$\frac{W}{W_0} = 1 - 4\Gamma\left(\frac{7}{4}\right)Nq\lambda_\beta\sqrt[4]{\frac{3\delta m\nu_\beta^2 T}{2e^2F^2}}, \tag{1.11}$$

where $\nu_\beta = Nq\sqrt{2T/M}$. W/W_0 increases with F/N because the average electron wavelength decreases.

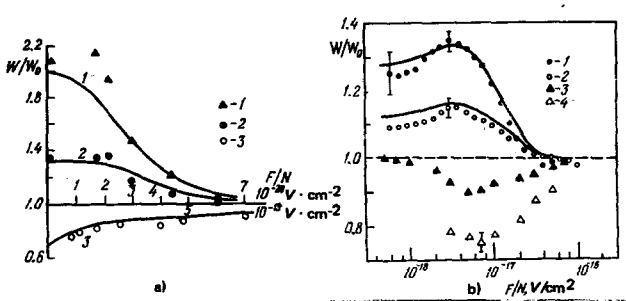

FIG. 3. Reduced drift velocity of electrons in dense gases vs. F/N ($T = 300$ K). a) Argon: 1) $N = 2.5\cdot10^{21}$ cm^{-3}; 2) $1\cdot10^{21}$ cm^{-3}; hydrogen: 3) $N = 1\cdot10^{21}$ cm^{-3}; b) methane: 1) $N = 1.1\cdot10^{21}$ cm^{-3}; 2) $0.5\cdot10^{21}$ cm^{-3} [17]; ethane: 3) $N = 1.1\cdot10^{21}$ cm^{-3}; 4) $0.4\cdot10^{21}$ cm^{-3}.[33]

Figure 3a compares calculated results[34] (curve 3) with experimental data obtained[14] in hydrogen at $T = 300$ K.

The results of a calculation according to (1.11) and (1.5) have been compared[18b] with experimental data obtained in helium at $T = 4.2$ K. The changes in electron drift velocity can be traced in Fig. 4 from "cold" to very "hot." Electron mobility is strongly suppressed by the interference effect at small F/N. Schwartz notes that relation (1.5) describes this state well, even though we might expect higher powers of the parameter $(\lambda_\beta qN)$ to appear in it. Only when the electrons are heated to an energy $\bar{\varepsilon} \approx 0.02$ eV (Fig. 4) are they free in the full sense of the word.

Figure 3a compares the results from measurements in argon with theoretical data (curves 1 and 2) obtained with the use of (1.8), which corresponds to the case of high polarizability.[34] The ratio W/W_0 decreases with increasing F/N as the average electron energy increases. An increasing fraction of the electrons enters the energy range in which the density corrections are small, i.e., the range of energies exceeding the energy of the Ramsauer minimum. It is obvious that competition between these two effects may also produce a nonmonotonic W/W_0 curve. This is the situation in methane, where both of the effects have been found to be important.[34] The calculated curves, constructed with account of these effects, and with consideration of the strong effect of the excitation of molecular vibrations on the distribution function, describe the experimental data accurately (see Fig. 3b).

c) Capture of electrons by molecules of the gas

Let us consider the drift of an electron in the case in which it can form a bound state with gas molecules as it moves. This hypothesis was made in Ref. 36 and discussed in Ref. 32. Since a negative ion has low mobility, we may assume that the electron moves only in those intervals of time in which it is free. We then have for the reduced mobility

$$\frac{\mu}{\mu_0} = w_e,$$

where w_e is the probability that the electron is free. It is most probable that the bound states are self-ionization states and arise on excitation of rotational (or vibrational) states of the molecule by the electron.

Let us assume that the electron makes many transi-

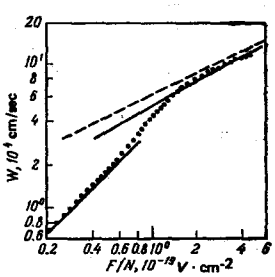

FIG. 4. Experimental values of drift velocity in helium at $T = 4.2$ K ($N = 0.948\cdot10^{21}$ cm^{-3}).[18b] The dashed line is the drift velocity W_0 in the ideal-gas approximation; the upper solid curve was computed with (1.11), the lower one with (1.5).

tions from the bound state to the free state and back as it drifts between the electrodes.[37] This condition is satisfied with a comfortable margin under actual experimental conditions. Then $w_e(1-w_e)=n_b/n_f$, where n_b and n_f are the densities of the free and bound electrons at static equilibrium. This yields[37]

$$\frac{\mu}{\mu_0}=\frac{1}{1+N\mathcal{F}}. \tag{1.12}$$

If the electrons are thermalized, $\mathcal{F}$ is given by the Saha formula $\mathcal{F}\approx\lambda_\varepsilon^3\exp(-\varepsilon_a/\bar{\varepsilon})$, where ε_a is the excitation energy of the self-ionized state and $\bar{\varepsilon}$ is the average electron energy, in this case T. Since the equilibrium is only relative in the heating field, $\mathcal{F}$ acquires a more complex form:

$$\mathcal{F}=\frac{\pi^3\sqrt{2}\hbar^3}{m^{3/2}}f(\varepsilon_a), \tag{1.13}$$

where $f(\varepsilon_a)$ is the electron energy distribution function at $\varepsilon=\varepsilon_a$. For example, for a molecule whose cross section is independent of energy we have $\mathcal{F}\approx\lambda_\varepsilon^3\exp(-\varepsilon_a^2/2\bar{\varepsilon}^2)$. Since $f(\varepsilon_a)$ is largest if the average energy $\bar{\varepsilon}$ is equal to ε_a, it follows from (1.12) and (1.13) that μ/μ_0 has a minimum at $\varepsilon=\varepsilon_a$, irrespective of the specific form of $f(\varepsilon)$. This permits inferences as to ε_a on the basis of experimental data. We note also that while the interference correction is determined by the small parameter λqN, the correction considered here is characterized by the parameter λ^3N (provided that $\bar{\varepsilon}\approx\varepsilon_a$). It may therefore be more important at small $\bar{\varepsilon}$.

This situation obviously obtains in a number of molecular gases (the mechanism does not operate in atomic gases[32]). The minimum of μ/μ_0 is quite distinct in C_2H_6 (see Fig. 3b); we find that $\varepsilon_a\approx 0.08$ eV. Electron capture at low F/N can also be assumed from measurements[38] made in H_2 at $T=77$ K. The measured $W/W_0(F/N)$ curves have a nonmonotonic trend whose details cannot be described by the interference correction.

It was observed in Ref. 37 that the situation may be more complex in reality. At large N, ε_a may itself depend strongly on N as a result of a shift of the continuum boundary. Then the density parameter λ^2LN, which determines this shift due to the interaction of electrons with gas atoms, may become important.

d) Mobility at high densities

Although the experimental material is far from exhaustive, there is reason to believe that the behavior of electrons at moderate densities anticipates the phenomena that arise at still higher densities N. The reduced mobility μ/μ_0 in He drops sharply in the critical density range as a result of localization of electrons—trapping of the particles in massive "bubbles." This effect is discussed in detail in Sec. a) of Chap. 2 and is illustrated in Fig. 8. In Ar, on the other hand,—even in liquid argon—the electron remains free, with a high mobility in the hundreds of cm^2/V sec.

Let us first consider the situation in Ar.[21] The solid curves in Fig. 5 are density curves of the scattering amplitude in the medium, $f(N)$, extracted from

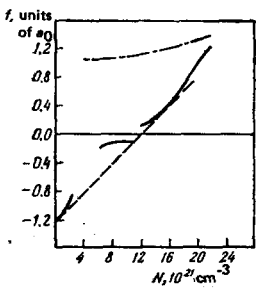

FIG. 5. Effective amplitude of scattering of electron on Ar atom vs. density of gas[16] and liquid.[22] The dashed curve is the theoretical relation.[21]

measurements of mobility in gaseous[16] and liquid[22] argon. It is known that the scattering amplitude in matter may not only acquire corrections, as has been demonstrated in the foregoing sections, but may also depart radically from the scattering amplitude on an isolated particle or even change sign (see, for example, Ref. 39). This is precisely the situation in argon, as was pointed out by Lekner in his papers on electron mobility in the liquid.[20,40] We shall discuss the situation in simpler terms, working from the potential (1.7).

The dashed line in Fig. 5 is the $f(N)$ relation corresponding to scattering on the potential (1.7). Expression (1.8) is valid for $f(N)$ at small N. The scattering amplitude decreases in absolute value as a result of weakening of the polarization component of the potential. It then passes through zero and begins to increase. At very large N, it may reach the value $L_1=L-(\pi/4)\alpha/a_0r_0$, which would indicate scattering on an unpolarized atom. Naturally, repulsion predominates in this case.

The actual situation is much more complicated at liquid densities. The structure of the medium becomes very important. The squared scattering amplitude is multiplied by the structure factor $S(0)$[41]:

$$S(0)=1+N\int[g(r)-1]\,d\mathbf{r}=NT\varkappa, \tag{1.14}$$

where $g(r)$ is a pair function of the interatomic correlation and $\varkappa$ is the isothermal compressibility of the medium. $S(0)\approx 1$ in a gas, and is of the order of a few hundredths in simple liquids in the neighborhood of the triple point.

At first, the decrease in $|f(N)|$ and then the decrease of the structure factor $S(0)$ maintain mobility on a high level. The electron remains free in liquid argon.

In contrast to the case of argon, the reduced mobility μ/μ_0 in helium increases with increasing density N of the gas in accordance with (1.5). The mobility vanishes if we let the parameter λqN tend to unity. This is a qualitatively correct result, since electrons in very dense (and liquid) helium are "trapped" in "bubbles," having a mobility of ~0.1 $cm^2/V\cdot sec$. This extrapolation, of course, is not legitimate. However, we note that the condition $\lambda=l$, where l is the free path, is the trapping criterion proposed by Mott.[42] It will be shown in Sec. c) of Chap. 2 that the condition $\lambda qN=1$ is indeed a criterion for localization on small density fluctuations.[43]

e) Annihilation of slow positrons in moderately dense inert gases

The positron annihilation rate λ_1 in matter is governed by the interaction of the positron with electrons on the atoms of the media. At low densities, λ_1 is proportional to the concentration N of the gas atoms[3]:

$$\lambda_1 = \pi r_0^2 c N Z_{\text{eff}}, \tag{1.15}$$

where $r_0 = e^2/mc^2$ is the "classical radius" of the electron, c is the velocity of light, and Z_{eff} is the effective number of electrons per atom of the gas. Z_{eff} is about equal to the charge Z of the nucleus if the wave function of the positron is not disturbed very much on scattering of the positron on a gas atom, i.e., if the interaction between them is small.

Anomalously large values of Z_{eff} have been observed in many rarefied gases and have been shown[44] to result from the formation of bound states between the positron and an atom (molecule) of the gas. This and other related phenomena have been discussed in detail in the reviews.[3,45] Below we shall consider density effects observed in inert gases, where the formation of bound states is impossible and the positron remains free. Several investigators have observed deviations (exceeding the limits of experimental error) from the linear law $\lambda_1 \sim N$ in these gases. We assume that these deviations are related to density effects in the mobility of slow electrons.

Let us discuss the experimental data. The annihilation rate has been determined by reducing measurements of the lifetimes of a large number of emitted positrons in the medium. The lifetime of each was measured by detecting two gamma quanta. The first was emitted as a result of emission of a positron, while the second was one of those emitted upon annihilation. Reduction of annihilation time spectra (see, for example, Ref. 3) gives the characteristics of a number of phenomena, including the value of λ_1. It appears in the argument of the exponential $\exp(-\lambda_1 t)$, which approximates one of the short-lived components of the time-distribution curve of positron annihilation (Fig. 6).

Some of the positrons that enter the medium form light positronium atoms even before they are thermalized. These positrons are also annihilated with time. The annihilation rate of ortho-positronium can be represented in the form

$$\lambda_2 = \lambda_v + \Delta\lambda_2, \quad \Delta\lambda_2 = 4\pi r_0^2 c Z_{\text{eff}}^1 N. \tag{1.16}$$

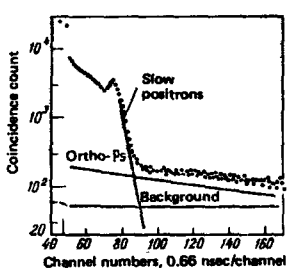

FIG. 6. Time spectrum of positron annihilation in He[4,46] at $T = 5.5$ K ($\rho = 0.023$ g·cm^{-3}). The positronium and orthopositronium (ortho-Ps) components and the background are indicated.

As $N \to 0$, λ_2 tends to the vacuum value $\lambda_v = 7.2 \cdot 10^6$ sec^{-1}. The annihilation pick-off rate (or "quenching" rate) $\Delta\lambda_2$ is governed by the interaction with electrons of the medium. Z_{eff}^1 is the effective number of electrons per gas atom that are in the singlet state with respect to the spin of the positron in the Ps atom. The same time spectra of annihilation are used to determine $\lambda_2(N)$. A nonlinearity in the variation of $\lambda_2(N)$ has been observed at large N in certain studies. It is of equal interest to us as the same effect in $\lambda_1(N)$. In the nature of its interaction with atoms of the gas, positronium is closely similar to the electron in helium in that it has a positive scattering length L of the order of a_0.

The results of annihilation-rate measurements for ortho-positronium in dense helium appear in Fig. 7. Deviations from linearity appear at $T = 77$ K, beginning at $N \approx 5 \cdot 10^{21}$ cm^{-3},[30,47,48] and increasing with increasing N. These deviations lower the annihilation rate noticeably.

Much weaker but systematic density effects have also been observed in the annihilation of positrons. In Ref. 48, $\lambda_1(N)$ began to increase at a rate somewhat lower than N in helium at 77 K at $N \gtrsim 8 \cdot 10^{21}$ cm^{-3}. On the other hand, $\lambda_1(N)$ increases more rapidly, beginning at $N \approx 3 \cdot 10^{20}$ cm^{-3} in krypton at 300 K.[49]

A number of authors have discussed the factors leading to the nonlinear variation of annihilation rate usually in connection with experiments on Ps.[30,47,48,50,52] The formation of positronium bubbles is not yet possible under the conditions of these experiments; see Sec. b) of Chap. 2. The cause of the anomaly may be scattering on several atoms[50] or an excluded-volume effect.[29,30] The latter is less significant in gases because it is determined by the parameter $(32\pi/3)L^3N$. The value of this parameter is 0.084 at $N = 5 \cdot 10^{21}$ cm^{-3}, since $L = 1.5a_0$. As for the first-named effect, it also lowers Z_{eff}^1 by further disturbing the wave function of the scattered positronium, and is determined by the parameter λqN (see Chap. 1, Sec. a). The value of this parameter is 0.64.

Let us discuss the anomalies in λ_1. Z_{eff} decreases in helium, apparently for the same reason. The parameter λqN is 0.07 at $N = 8 \cdot 10^{21}$ cm^{-3}, since $L = -0.45a_0$. Because of the small value of the param-

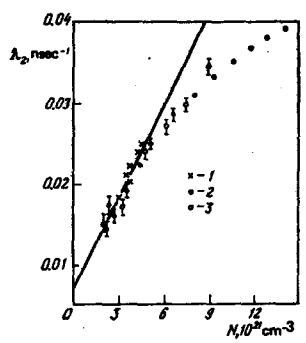

FIG. 7. Orthopositronium annihilation rate vs. helium density. Plotted points: 1) from Ref. 48 for $T = 300$ K; 2 and 3) from Refs. 48 and 30 at 77 K; the line corresponds to $Z_{\text{eff}} = 0.125$ according to measurements[49] at small N.

eter, the observed deviation from linearity in $\lambda_1(N)$ is also small. The increase in Z_{eff} in krypton is apparently due to a polarization effect [(see Chap. 1, a)], which weakens the interaction of the positron with atoms of the medium. The parameter $4\pi^2\alpha^2N(3a_0r_0L)^{-1}$, which determines the magnitude of this effect,[34] is 0.037 if $L=-4a_0$ and $r_0=a_0$.

2. BOUND STATES OF ELECTRONS, POSITRONS, AND POSITRONIUM IN DENSE GASES

The phenomenon of self-trapping of light particles in matter has long been known in the physics of the condensed state.[53] One such particle is the polaron.[54] In a disordered medium, bound states of the electron (positron, positronium) are possible if the system gains free energy when there is competition between the electron binding energy in the density-fluctuation field and the work done to create the fluctuation.[5,55] Transition to the bound state occurs when the density rises or the temperature drops—either factor intensifies the interaction effect. The nature of the self-trapped (fluctuon) state depends on the nature of the interaction between the electron and atoms (molecules) of the matter. If repulsive forces dominate, the electron is localized on a rarefaction fluctuation, and a "bubble" appears. If attraction predominates, trapping may occur on a condensation, with a "cluster" as the result. Formations of mixed type are also possible.[6]

Transition of electrons to the bound state has a radical influence on a number of properties of the matter. Positronium bubbles were the first to be observed, since the annihilation time of positronium in liquid helium was found to be several times larger than expected.[56,57] Anomalous behavior of electrons injected into liquid helium was observed almost simultaneously with the discovery of the uncommonly long lifetime of positronium.[58-60] The mobility of the electron was that of a massive formation (tens of M) and not that of a light particle. Ferrell[29] and Kuper[61] explained these effects. The strong exchange repulsion between positronium (the electron) and He atoms favors trapping of the light particle in a cavity. The cavity radius is 15–18 Å, and ~10^2 He atoms are displaced from it. The properties of bubbles in the liquid have been studied thoroughly.[61-65,7,28] Bubbles have been observed not only in helium, but also in several other nonpolar liquids.[66,67]

Study of self-trapped states in dense gases apparently began with the experiment of Levine and Sanders[68] to determine electron mobility in gaseous helium. Electron bubbles are discussed in Sec. a). The next Section b) is devoted to positronium bubbles and the annihilation of positronium in gases. Clusters can form in a dense gases if the polarizability of the atoms is high.[69,70] Section c) also discusses "orientation" clusters in a medium of dipolar molecules. Anomalies in the positron annihilation rate in a dense gas, which have been interpreted as a result of condensation of the gas around the positron, were first observed in Refs. 71 and 72. It was shown in Ref. 73 that positrons in dense gases go over to self-trapped states, a curve of the transition to the bound state was constructed, and the presence of a critical point for the clusterization phenomenon was predicted. Measurements[74a] have confirmed the theoretical estimates. These problems are discussed in Sec. d).

a) Electron bubbles in dense gases

Levine and Sanders[68] presented a convincing demonstration of the existence of electron bubbles in dense gaseous helium. The time-of-flight method was used to measure mobility as a function of helium density at $T=4.2$ K. It was found that the value of μ corresponds to the mobility of free electrons at low N, but approaches the mobility of electrons in liquid helium at high N. The $\mu(N)$ discontinuity occurs in a very narrow range: a density increase by only a small factor is accompanied by a mobility increase of more than five orders of magnitude (Fig. 8). Levine and Sanders also submitted a qualitative explanation of this effect.[76] They assumed that the electrons are trapped in bubbles at high densities, as is the case in liquid helium. As the density is lowered, formation of bubbles becomes less favored, and all electrons are free at low densities. Their mobility may be several orders higher than the mobility of the bubbles.

If trapping is possible, the ratio of the free-electron concentration n_f to the trapped concentration n_b is determined by the magnitude and sign of the system free energy change ΔF caused by a single trapping event:

$$\frac{n_f}{n_b}=A\exp(\beta\Delta F). \tag{2.1}$$

Determination of the ΔF in the argument of the exponential is the main task of the theory of self-trapped electron states. Generally speaking, the average over all possible atom configurations that realize trapped electron states should appear in the right-hand side of (2.1). In first approximation, however, it is sufficient to use only the optimum atom-concentration fluctuation, i.e., that which causes the largest decrease in system free energy as a result of electron trapping. The result will be the more accurate the deeper and wider (and, consequently, the more improbable) the optimum fluctuation that realizes the particular state.

The multiplier A applied to the exponential in (2.1)

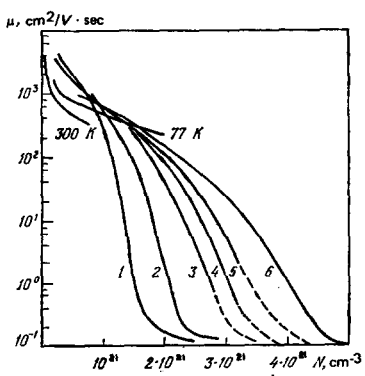

FIG. 8. Dependence of electron mobility μ on density N in dense gaseous helium. Temperatures, $T(K)$: 4.2 (1), 7.3 (2), 11.6 (3), 13.8 (4), 18.1 (5)[75] and 20.3 (6).[26]

takes the translational, rotational, and vibrational degrees of freedom of the bubble into account. It is very difficult to compute it properly, for essentially the same reasons that obtain in determining the concentration of new-phase nuclei in nucleation theory. It is usually assumed that this multiplier is of the order of unity and depends weakly on the density and temperature of the gas as compared to $\exp(\beta\Delta F)$.

Below we derive conditions for the appearance of bubbles and their principal parameters, make a comparison with experiments, and discuss certain more complex problems.

1) *Elementary model.* Let us assume that an electron is trapped in a spherical cavity of radius R that contains no helium atoms (the "empty square well" model).[76-78] Then

$$\Delta F = -\varepsilon(R) + \frac{4\pi}{3} R^3 p, \tag{2.2}$$

where $\varepsilon(R)$ is the electron binding energy and p is the gas pressure. The second term in (2.2) corresponds to the work that must be done to create the cavity.

The free electron is in the average field of the atoms surrounding it, a field whose magnitude is $2\pi\hbar^2 NL/m$ in the optical-pseudopotential approximation; here L is the electron-on-atom scattering length.[79] The binding energy of the trapped electron is smaller than this value by the energy of its vibrations in the bubble. The latter is well known for the square well.[80] We shall assume for simplicity that there are several levels in the bubble. Then $\varepsilon(R) \approx (2\pi\hbar^2 NL/m) - (\pi^2\hbar^2/2mR^2)$. The optimum bubble size R_0 can be obtained from the condition minimizing ΔF:

$$R_0^5 \approx \frac{\pi\hbar^2}{4mp}. \tag{2.3}$$

If we neglect the role of the multiplier before the exponential in (2.1), we can easily obtain a simple relation between the density N_{cl}, the pressure p_{cl}, and the temperature T_{cl} on the line of transition of the electrons from the free to the trapped state, which it is natural to determine with the condition $\Delta F(R_0) = 0$. We obtain

$$\frac{\hbar^2 N_{cl} L}{m p_{cl}^{2/5}} = \frac{5}{3}\left(\frac{\pi}{4}\right)^{3/5}. \tag{2.4}$$

In a sufficiently rarefied gas, $p = NT$,

$$N_{cl} L^{5/3} \lambda_\beta^{4/3} = c, \quad R_{cl}^3 = \frac{6}{5} L\lambda_\beta^2, \tag{2.5}$$

where $\lambda_\beta = \hbar/\sqrt{2mT}$ is the thermal wavelenfth of the electron and $c = \pi(5/3)^{5/3} \cdot 2^{-8/3} \approx 1.16$. This relation between N_{cl} and T_{cl} was obtained in Refs. 78, 81.

In He^4, where $L = 0.62$ Å, relation (2.5) with $T_{cl} = 4.2$ K gives $N_{cl} = 5.2 \cdot 10^{21}$ cm^{-3}. This value is correct in order of magnitude, and, more importantly, the qualitative dependence $N_{cl} \sim T_{cl}^{2/3}$ is also correct. The latter statement follows from Fig. 9, which was obtained by processing the data shown in Fig. 8.

Quantitative agreement with experiment cannot be required of such a simple model. This is because some of the assumptions were poorly based. Thus, we assumed that the vibrational energy of the electron was small in the ground state of the bubble as compared to

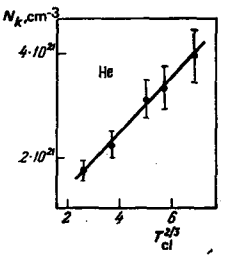

FIG. 9. $N_{cl}(T)$ plot. The circles represent experiment.[26,75].

the potential barrier height ($4NLR_0^2/\pi \gg 1$. Actually, we find that $4NLR_0^2/\pi = 5/3$. This indicates that the exact expression must be used for $\varepsilon(R)$. Here relation (2.5) holds, but the constant c is reduced in the necessary direction, $c \approx 0.59$.[78]

The model is simple to use because the dependence of ε on R is known. The models discussed in Refs. 23, 26, 75, 82, and 83, where similar results were obtained, have the same advantage. The shape of the well was also postulated in these papers. Actually, it should be determined by self-consistent solution of the problem.

2. *The self-consistent-field approximation.* The complete derivation of the self-consistent-field expression can be found in Refs. 5, 6, 43, 76. Here we write them out on the basis of simple qualitative considerations.

Let us consider, in the classical limit, the free energy F of the system formed by an electron in an ideal gas. The part of F due to the interaction is $NT\int d\mathbf{r}(1 - e^{-\beta V})$, where N is the density of the atoms and $V(\mathbf{r})$ is the electron-atom interaction potential. In the absence of correlation between the electron and the atoms, this quantity would equal $N\int V(\mathbf{r})\,d\mathbf{r}$. Thus, the change ΔF in system free energy due to the appearance of correlation in the positions of the atoms equals

$$\Delta F = -NT\int [e^{-\beta V(\mathbf{r})} - 1 + \beta V(\mathbf{r})]\,d\mathbf{r}. \tag{2.6}$$

The generalization of this expression to the quantum case is obvious. First, $V(\mathbf{r})$ must be replaced by $\tilde{V}(\mathbf{r}) = \int V(\mathbf{r} - \mathbf{r}')|\psi(\mathbf{r}')|^2 d\mathbf{r}'$, where ψ is the wave function of the trapped electron. Second, it must be recognized that the average value of the electron's kinetic energy is nonzero because of the zero-point vibrations. This gives

$$\beta\Delta F = \lambda_\beta^2 \int |\nabla\psi(\mathbf{r})|^2 d\mathbf{r} - N\int [e^{-\beta\tilde{V}(\mathbf{r})} - 1 + \beta\tilde{V}(\mathbf{r})]\,d\mathbf{r}. \tag{2.7}$$

Accordingly, the distribution of the atoms around the electron is given not by the expression $N(\mathbf{r}) = N\exp(-\beta V)$, but by the more complex

$$N(\mathbf{r}) = Ne^{-\beta\tilde{V}(\mathbf{r})} = N\exp\left[-\beta\int V(\mathbf{r} - \mathbf{r}')|\psi(\mathbf{r}')|^2 d\mathbf{r}'\right]. \tag{2.8}$$

Now to answer the question as to the possibility of electron trapping it is necessary to find the wave function of the electron in the self-consistent potential $\int V(\mathbf{r} - \mathbf{r}')[N(\mathbf{r}') - N]d\mathbf{r}'$. This self-consistent equation is typical for the theory of trapped states in disordered systems. It is a particular case of the optimum-fluctuation method proposed in Refs. 11, 12, 84 and widely used in the theory of condensed disordered sys-

tems.[4,6,9,85] Analytic solution of the above equations is evidently impossible because the form of the potential $V(\mathbf{r})$ is not known for all atoms and the equations are also nonlinear.

The problem is greatly simplified for gases whose atoms have low polarizability (for example, helium) and if the electron wavelength is considerably larger than the effective radius of the electron-atom forces. The pseudopotential (1.3) can then be used for $V(\mathbf{r})$. This gives for $\tilde{V}(\mathbf{r})$

$$\tilde{V}(\mathbf{r}) = 2\pi\hbar^2 L\,|\psi(\mathbf{r})|^2 m^{-1}. \tag{2.9}$$

We shall seek the solution by the direct variational method.

We use the simplest approximation for the wave function of the electron ground state in the bubble:

$$\psi(\mathbf{r}) = \left(\frac{2}{\pi\lambda^2}\right)^{3/4} \exp\left(-\frac{r^2}{\lambda^2}\right). \tag{2.10}$$

This trial function is exact for the ground state of an oscillator. It is hoped that the relation (2.10) is a good approximation. After substitution of (2.10) into (2.9) and (2.7), ΔF becomes a function of only the single parameter λ, the wavelength of the electron in the bubble:

$$\beta\Delta F = 3\frac{\lambda_\beta^2}{\lambda^2} - \left(\frac{\pi}{2}\right)^{3/2} N\lambda^3 \sum_{n=2}^{\infty} (-1)^n \frac{B^n}{n!\, n^{3/2}}, \tag{2.11}$$

where

$$B = 8\sqrt{\frac{2}{\pi}}\frac{L\lambda_\beta^2}{\lambda^2}. \tag{2.12}$$

As in the square-well model, the optimum bubble size λ_{cl} and the relation $N_{cl}(T_{cl})$ between the density of the gas and the temperature on the transition line can be obtained without difficulty from the conditions $\Delta F = 0$ and $\partial\Delta F/\partial\lambda = 0$. This relation is the same as (2.5), except that the constant $c \approx 0.42$. At $T_{cl} = 4.2$ K, $N_{cl} = 1.9 \times 10^{21}$ cm^{-3}, which is now very close to the density at which the electron-mobility jump is observed (Fig. 8).

The results obtained are valid if the conditions for use of the optical pseudopotential, $L \ll \lambda_{cl}$ and $N_{cl}L^3 \ll 1$, and the macroscopic-bubble condition $N_{cl}\lambda_{cl}^3 \gg 1$, are satisfied. Using expression (2.5), we see that they are satisfied on the transition line if $L \ll \lambda_\beta$. We shall give some estimates. At $T_{cl} = 4.2$ K, we have $\lambda_\beta = 100$ Å, the optimum bubble size $\lambda_{cl} = 25$ Å, and the number of displaced atoms is greater than one hundred. The theory is therefore valid.

3) *Principal characteristics of bubbles.* Figure 10 shows typical bubble-density profiles in He^4 at $T = 7.3$ K. The bubble size ($R \approx 25$ Å) decreases somewhat with increasing N at constant temperature, and its shape becomes more and more square. The residual number of atoms inside the bubble decreases. Under the same conditions, the electron binding energy in the bubble changes from 0.07 eV at $N = 2.5 \cdot 10^{21}$ cm^{-3} to 0.1 eV at $N = 5 \cdot 10^{21}$ cm^{-3}. Optimum bubbles contain two or three levels. This indicates that the classical description of trapped electron states that was used in Refs. 86–89 is invalid. Another critique of those

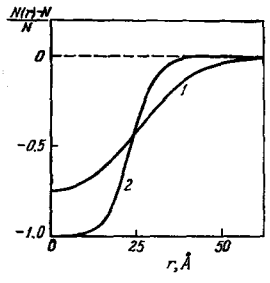

FIG. 10. Concentration of He^4 atoms within bubble vs. distance to center of bubble at $T = 7.3$ K. Curve 1: $N = 2.5 \cdot 10^{21}$ cm^{-3}; curve 2: $5 \cdot 10^{21}$ cm^{-3}.

papers will be found in Ref. 90.

Optical experiments are of great importance for determination of electron-state structure in bubbles. No such experiments have as yet been reported in gases. In liquid helium, a current jump (and hence also a mobility jump) has been observed under exposure to electro-magnetic radiation.[91] This effect is governed by photoionization of the bubbles. Figure 11 shows the level of the detected signal as a function of photon energy $\hbar\nu$.[91] The maximum at $\hbar\nu \approx 0.9$ eV corresponds to photoionization of the bubble, and the one at $\hbar\nu \approx 0.7$ eV to the $1s - 3p$ transition.[91,92] The possibility of direct optical absorption and Raman scattering of light by bubbles has also been investigated theoretically.[93,94] Estimates showed that reliable registration of these effects requires an electron concentration of the order of 10^{12} cm^{-3}. Such concentrations are not yet attainable in actual experiments.

Figure 8 showed plots of injected-electron mobility vs. density. A mobility jump occurs at low temperatures, so that the bubble-formation density N_{cl} is measured automatically. The transition becomes smoother at high T. Measurements of $\mu(N)$ were made in Refs. 23–26 at high temperatures, $20 < T < 160$ K. We shall dwell only briefly on the mobility problem, since it was discussed in Shikin's review.[63]

When both free and bound electrons are present in the transitional range, we can write for μ[95]

$$\mu = \frac{\mu_f n_f + \mu_b n_b}{n_f + n_b}, \tag{2.13}$$

where μ_f and μ_b are the mobilities of the free electrons and the bubbles. We note first of all that the gaskinetic approximation becomes invalid for μ_f at these densities (Sec. 1). The first attempt to measure μ_f under conditions such that electrons "of both species" are present was made in Ref. 96. The $\mu_f(N)$ relation becomes more nearly exponential, but it is

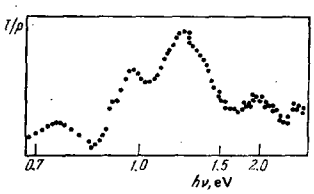

FIG. 11. Detected-signal level I/p vs. electron energy[91] (I is the detected current and p is the light flux).

much smoother than $\mu(N)$. Theoretical investigation of $\mu_f(N)$ would be of definite interest, since the studies made thus far[86,87,97-99] have not yet produced a solution to this problem.

The Stokes approximation is known to work quite well for the mobility of bubbles in liquid He. Its use is also justified in gases at high N. The Knudsen approximation could be used in more rarefied gases. However, an intermediate regime obtains at the transition densities and we have nothing better than the interpolation formula[76]

$$\mu_b^{-1} \approx \mu_c^{-1} + \mu_{cl}^{-1}, \quad \mu_c = \frac{e}{6\pi\eta R}, \quad \mu_{cl} = \frac{3e}{8NR^2\sqrt{2\pi MT}}, \qquad (2.14)$$

where R is the radius of the bubble, η is the viscosity of the gas, and M is the mass of the atom. These expressions do not take account of the excitation of internal degrees of freedom, which may occur when the bubble interacts with the medium.

The surface of the bubble may vibrate. The presence of excited vibrations may be significant in determining the ratio n_f/n_b: it may broaden electron levels, promote relaxation of the electrons into trapped states, and influence mobility. Bubble vibrations in liquid He were discussed in Refs. 94, 100, 101. Naturally, the spherical mode has the smallest vibrational quantum $\hbar\omega$. Analysis of the vibrations of an electron-containing cavity in a gas leads to the expression

$$\omega^2 = \frac{1}{4\pi MNR_0^4}\frac{\partial^2 F}{\partial R^2}\Big|_{R=R_0}, \qquad (2.15)$$

where $F(R)$ is, as before, the free energy. It is natural to call $2\pi NR_0^3M/3$ the effective mass m^* of the bubble. It is the same as the apparent mass in the hydrodynamic approximation. It can be estimated by using the known value of the apparent mass of a bubble in a dense medium, which equals half the mass of the displaced atoms,[79] for m^*: $m^* \approx 2\pi NR_0^3M/3$ where M is the mass of an atom of the gas. In liquid helium, these values of m^* agree with measurements: $m^* \approx 100M$.[102] On the transition line in a gas at $T = 4.2$ K, $m^* = (2\pi/3)MN_{cl}R_0^3 = 32M$. The quantity m^* was measured indirectly in Ref. 103 and found to be surprisingly small: $3 \leq m^*/M < 5$. This result remains unexplained.

Let us rewrite (2.15) in the form

$$\omega^2 = 5T(MR_0^2)^{-1}.$$

At $T = 4.2$ K and $N = 1.5 \cdot 10^{21}$ cm^{-3} we have $\hbar\omega \approx 0.8$ K. These vibrations are therefore excited. However, as is usually assumed, they are unimportant in the exponential multiplier of (2.1).

Surface tension in the liquid is a significant factor. The surface free energy ΔF_s, defined as the excess free energy associated with the missing neighbors of surface-layer particles,[104] competes in the expression for ΔF with the change in the volume free energy $\Delta F_g = (4\pi/3)pR^3$. There is no surface energy at all in a rarefied gas, and in a moderately dense gas it can be expressed in terms of the second virial coefficient $B(T)$:

$$\beta\Delta F_s = -(4\pi R^2)N_sNB,$$

where $N_s \approx N^{2/3}$ is the surface density of the atoms.

Comparing ΔF_s with ΔF_g, we see that these effects are of little importance in a gas because

$$\frac{\Delta F_g}{\Delta F_s} = \frac{RN^{1/3}}{NB} \gg 1.$$

b) Positronium bubbles and positronium annihilation rate

Electron bubbles are formed as a result of strong exchange repulsion between the electrons and atoms of the gas (the role of the polarization interaction is small). Therefore everything that was said above concerning electron bubbles can be extended directly to positronium bubbles, since the interaction of positronium with gas atoms is also of repulsive nature. Thus, for example, the temperature dependence of the gas density N_{cl}^{Ps} at which the formation of positronium bubbles comes to be favored is easily expressed in terms of the analogous quantity N_{cl} obtained for electrons (2.5):

$$N_{cl}^{Ps}(T) = 2^{2/3}\left(\frac{L_e}{L_{Ps}}\right)^{5/3} N_{cl}(T); \qquad (2.16)$$

here L_e and L_{Ps} are the scattering lengths of the electron and the positron on the atom and it has been recognized that positronium has a mass of $2m$. In helium, for example, where $L_e \lesssim L_{Ps}$ the regions of existence of electron and positronium bubbles practically coincide.

1) Positronium annihilation rate. The annihilation rate $\lambda_2(N)$ increases linearly with N or is weakly nonlinear (see Chap. 1, Sec. e)) under the conditions of weak interaction between the Ps and the gas atoms. Transition of Ps atoms to the bubble state results in qualitative changes in the $\lambda_2(N)$ relation (Fig. 12). The annihilation rate decreases sharply at $N \sim N_{cl}$ owing to rarefaction of the gas around the positronium. These effects were first observed in Refs. 71, 72 in gaseous He^4.

Let us discuss the $\lambda_2(N)$ relation with allowance for the possibility that the bubble may contain Ps. By analogy with (2.13), we can write the following expression for $\Delta\lambda_2$, the pick-off annihilation rate:

$$\Delta\lambda_2 = \frac{\Delta\lambda_f n_f + \Delta\lambda_b n_b}{n_f + n_b} = \Delta\lambda_f\left(1 + \xi\frac{n_b}{n_f}\right)\left(1 + \frac{n_b}{n_f}\right)^{-1}; \qquad (2.17)$$

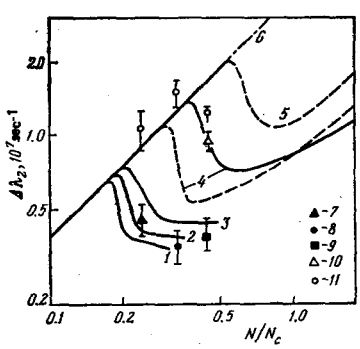

FIG. 12. Pick-off annihilation rate of positronium vs. reduced density in He^4. The solid curves represent the numerical calculation,[105] the dashed curves expressions (2.25) and (2.26). The plotted points represent the experiment of Ref. 46. Temperatures $T(K)$: 4.8 (1 and 7), 5.4 (2 and 8), 6.4 (3 and 9), 13 (4 and 10), 30 (5 and 11), and 300 (6).

here n_b/n_f is the ratio of the probabilities that the Ps is in the bound and free states and $\Delta\lambda_b$ and $\Delta\lambda_f$ are the corresponding quenching rates. In accordance with (1.16), $\Delta\lambda_f \sim N$. The expression for $\Delta\lambda_b$ is more complex:

$$\Delta\lambda_b = 4\pi r_0^2 c Z_{eff} \int N(\mathbf{r}) |\psi(\mathbf{r})|^2 d\mathbf{r}, \quad (2.18)$$

where $N(\mathbf{r})$ is the atom-concentration distribution in the bubble and $\psi(\mathbf{r})$ is the wave function of Ps in the bubble. Thus,

$$\xi = \frac{\Delta\lambda_b}{\Delta\lambda_f} = N^{-1} \int N(\mathbf{r}) |\psi(\mathbf{r})|^2 d\mathbf{r}. \quad (2.19)$$

Therefore the quenching rate (2.17) is determined by the relative quantities n_b/n_f and ξ. It can be calculated from the results of study of the positronium + gas system at equilibrium.

Let us use the results of the preceding section. According to (2.8), $N(\mathbf{r}) = N\exp(-\beta\tilde{V})$. Choosing the trial wave function $\psi(\mathbf{r})$ in the form

$$\psi(\mathbf{r}) = \sqrt{\frac{3}{2\pi\lambda^3}} \exp\left(-\frac{r^3}{\lambda^3}\right), \quad (2.20)$$

we obtain an expression for ξ:

$$\xi = \frac{1}{\beta\tilde{V}(0)}\{1 - \exp[-\beta\tilde{V}(0)]\}, \quad (2.21)$$

where $\beta\tilde{V}(0) = 6L\lambda_\beta^2/\lambda^3$, and λ is the wavelength of the trapped Ps. Naturally, λ is close to R_0 (2.3). The exact expression that corresponds to $\psi(\mathbf{r})$ (2.20) differs only in the numerical multiplier[105]

$$\lambda^5 = \frac{2^{2/3}\Gamma(1/3)}{2\pi} \frac{\hbar^2}{m_{Ps} p}, \quad (2.22)$$

where p is pressure of the gas and m_{Ps} is the mass of the positronium atom.

The expressions derived here can be used for qualitative analysis of the quenching rate $\Delta\lambda_2$ as a function of the density and temperature of the gas when $p = NT$. For example, let us consider $\Delta\lambda_2(N)$ on an isotherm. The formation of bubbles is not favored at low densities, and $\Delta\lambda_2 \approx \Delta\lambda_f \sim N$. When the density $N = N_{cl}$, $\Delta\lambda_2$ begins to decrease, assuming at $N > N_{cl}$ a value $\Delta\lambda_2 = \Delta\lambda_b = \xi\Delta\lambda_f$ that is a small fraction of $\Delta\lambda_f$ and then varying smoothly as N increases, $\Delta\lambda_2 \sim N^{2/5}$. This variation of $\Delta\lambda_2(N)$ agrees with observations (Figs. 12, 13).

2. Positronium annihilation rate in a nonideal gas. Recent experiments[46,106,107] on positronium annihilation were made in a broader range of densities than the experiments on electron mobility. At high densities, the gas can no longer be regarded as ideal, and it is necessary to consider the interaction among its atoms. Allowance for repulsion between atoms, which prevents bubble formation and may cause the bubbles to vanish completely, is most important.

We use a lattice-gas model to write the change in the free energy of the gas ΔF_g in the case of localization of positronium:

$$\beta\Delta F_g = \Delta S = \int \left[N(\mathbf{r}) \ln \frac{N(\mathbf{r})}{N} - \frac{1 - N(\mathbf{r})b}{b} \ln \frac{1 - N(\mathbf{r})b}{1 - Nb}\right] d\mathbf{r}, \quad (2.23)$$

where the constant b characterizes the interatomic repulsion. Minimizing the free-energy change $\Delta F = -\varepsilon + \Delta F_g$ with respect to $N(\mathbf{r})(\delta\Delta F/\delta N = 0)$, we obtain an expression for the distribution of atoms in the bubble:

$$N(\mathbf{r}) = N\exp[-\beta\tilde{V}(\mathbf{r})][1 + Nb\{\exp[-\beta\tilde{V}(\mathbf{r})] - 1\}]^{-1}. \quad (2.24)$$

In contrast to (2.8), this expression does not allow formation of a bubble at $Nb \to 1$.

Substituting (2.24) into (2.19) and integrating with the function (2.20), we obtain for ξ, which determines the positronium quenching rate, instead of (2.21)

$$\xi \approx -\frac{1}{Nb\beta\tilde{V}(0)} \ln[1 + Nb\exp[-\beta\tilde{V}(0)] - 1]. \quad (2.25)$$

Accordingly, we rewrite (2.22) in the form

$$\lambda = \left[\frac{2^{2/3}\Gamma(1/3)}{\pi} \frac{\lambda_\beta^2 b}{|\ln(1 - Nb)|}\right]^{1/5}. \quad (2.26)$$

At low densities ($Nb \ll 1$), expression (2.25) becomes the previous relation (2.21). The repulsive interaction between atoms of the gas, which tends to reduce the size of the bubble and increase the kinetic energy of the positronium and should therefore also increase $\Delta\lambda_2$, becomes important as the density increases. Relations (2.25) and (2.26) indicate that even at moderate densities $Nb \lesssim 1$, $\Delta\lambda_2 \sim |\ln(1 - Nb)|^{2/5}$ under the conditions of strong interaction, when $\beta\tilde{V}(0) \gg 1$.

In the limit of matter compressed to the maximum ($Nb \to 1$), ξ tends abruptly to unity and $\Delta\lambda_2 \to \Delta\lambda_f$. Therefore the bubbles vanish at high densities. This conclusion was obtained within the framework of a model that takes only the interatomic repulsion into account. It is also valid at high T, when the interatomic attraction has little influence, i.e., when $T_c N \ll T N_c$, where T_c and N_c are the critical parameters of the gas.

With the object of quantitative comparison with experiments, the annihilation rate was calculated in Ref. 105 from more accurate expressions for the free energy, which make it possible to take better account of the properties of the medium. Figure 12 presents the results of a numerical calculation of $\Delta\lambda_2$ for He^4. The best agreement with experiment[46] was obtained for the positronium-on-atom scattering length $L = 1.5a_0$. This value of L agrees well with the theoretical values obtained in Refs. 108–110.

The dashed curves in Fig. 12 were obtained by cal-

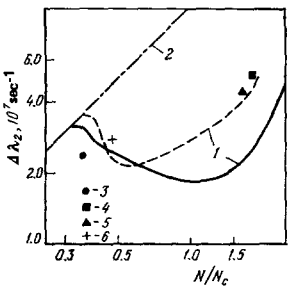

FIG. 13. Pick-off annihilation rate of positronium vs. reduced density in Ne. The solid curves represent numerical calculation,[105] the dashed curves relations (2.25) and (2.26), and the plotted symbols experiment.[106] Temperatures $T(K)$: 46 (1 and 3), 44 (4), 45 (5), 47.5 (6), and 300 (2).

culating $\Delta\lambda_2$ in the approximate model (2.25), (2.26). It conveys the qualitative features of $\Delta\lambda_2(N)$.

The annihilation rates of positronium in He^3 (Ref. 107) and Ne (Ref. 106) were recently measured. The observed effects indicate the presence of bubbles. Figure 13 shows the experimental data for Ne and the computed results of Ref. 105.

3) Trapping time. Up to this point, we have been considering the properties of bubbles in the state of thermodynamic equilibrium. The formation kinetics of bubbles is also of great interest. Here the most important characteristic is the time τ of bubble formation, i.e., the time of relaxation of the positronium (electron) from the free to the bubble state.

The relaxation time of positronium in liquid helium is in any event smaller than the annihilation time of para-positronium in a vacuum, $\tau_v \approx 10^{-10}$ sec. Para-positronium bubbles in liquid He have actually been observed and investigated.[111] They could not appear if $\tau < \tau_v$. Positronium must lose an energy $(E_1 - Ry/2)$ determined by the lower boundary of the Ore gap (E_1 is the ionization potential of the atom) within a time shorter than τ_v and transfer to a bound state with formation of a cavity. We do not now have a consistent kinetic theory of trapping, and for this reason we cite only a few qualitative considerations that permit inferences as to the order of magnitude of τ.

Positronium that forms in an atomic gas with an energy $\varepsilon > T$ is thermalized, losing energy in elastic collisions (if the ε are not very large). The thermalization time is of the order of $(2m/M)\sqrt{\varepsilon/2m}\,N^{1/3}$ considering that the free path in a dense medium is near $N^{-1/3}$. The thermalization time is around 10^{-11} sec if $N = 2 \cdot 10^{21}$ cm^{-3} and $\varepsilon = 1$ eV. If $N \leq N_{cl}$, thermalized Ps atoms are trapped. Let us estimate this time τ on the basis of a concept in which this process has two steps, $\tau = \tau_1 + \tau_2$.

At the first step, the positronium, situated in a fluctuation field with a density defect, $n = N(r) - N < 0$, is thermalized. We again estimate the deceleration time from the losses in elastic collisions, $\tau_{-1}^{1} = (2m/M)\sqrt{T/m}\,N^{1/3}$, which gives $\tau_1 \approx 10^{-10}$ sec at $T = 4.2$ K and $N = 2 \cdot 10^{21}$ cm^{-3}. Actually, τ_1 may be smaller because of energy losses in inelastic collisions, which excite fluctuation vibrations, etc. The time τ_1 should be smaller than or equal to the fluctuation lifetime $\tau_f \approx R^2/6D$, where R is the dimension of the fluctuation and D is the diffusion coefficient of the gas. There is always a small Gaussian fluctuation, but those that are most interesting are the ones that have one energy level for positronium, say a weakly bound one. Then size of the fluctuation is related to n by $R \approx (2\pi Ln)^{-1/2}$, $n = (3N/4\pi R^3)^{1/2}$. This makes it possible to estimate $\tau_f \approx 10^{-10}$ sec under the same conditions.

The second trapping step corresponds to formation of a cavity. After the positronium has lost its energy (and perhaps been trapped on a weakly bound level), the medium begins to receive pressure from it. The time τ_2 can be estimated as the time of expansion of the cavity at the speed of sound or the thermal velocity: $\tau_2 = R_0/u$. This gives $\tau_2 \approx 10^{-11}$ sec. According to these rough estimates, therefore, $\tau \lesssim 10^{-10}$ sec in gaseous helium.

A time of the same order is also necessary for formation of an electron bubble after injection of electrons into a gas. Accordingly, we shall discuss the measurements of Refs, 112–114, from which we can estimate the electron thermalization times in hydrogen and helium. In these experiments, the cathode emitted electrons with energies of ~1 eV, which then drifted toward the anode under the action of a weak applied field. The cathode and anode were separated by an energy barrier formed by image forces and by this field. If the electrons were thermalized before reaching the barrier, they did not reach the anode. Figure 14 shows plots of the thermalization times against N; they are of the order of 10^{-12} sec. The question as to why the thermalization time decreases more rapidly than $1/N$ remains open. This may result from the appearance of new vibrational degrees of freedom in dense matter.[112]

Some information on the kinetic processes can also be found in Refs. 115–117.

4) Energy barrier on surface of medium. The formation of bubbles is associated with a positive shift of the boundary of the continuous spectrum of the positronium (electron) in the gas:

$$E_B = \frac{2\pi\hbar^2 NL}{m}. \tag{2.27}$$

This formula, which is apparently due to Lenz,[118] is exact for a rarefied gas if $NL^3 \ll 1$. It becomes necessary to consider interatomic correlation as the density increases, and this gives the expression[119,120]

$$E_B = 2\pi\hbar^2 NLm^{-1}\left(1 - NL\int \frac{g(r)-1}{r}\,dr\right), \tag{2.28}$$

where $g(r)$ is the pair correlation function. If we take interatomic repulsion into account, assuming that $g(r) = 0$ at $r \leq r_a$ and $g(r) = 1$ at larger r, relation (2.28) gives

$$E_B = 2\pi\hbar^2 LNm^{-1}(1 + 2\pi NLr_a^3). \tag{2.29}$$

Expression (2.29) becomes invalid at large values of the parameter NLr_a^2.

An alternative approximation that can be used in dense matter, when $r_a \approx r_s$ (r_s is the interparticle distance and $(4\pi/3)Nr_s^3 = 1$), is the Wigner-Seitz approximation.[28,121] The electron is considered in a medium that is broken down into equivalent spheres of radius

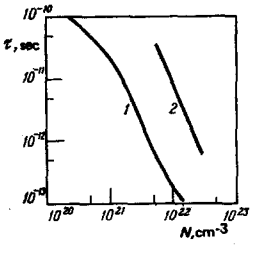

FIG. 14. Thermalization time of hot electrons as a function of gas density. 1) hydrogen; 2) helium.[112,114]

r_s, each of which contains a solid sphere of radius L ($L<r_s$) at its center. The electron also has a nonzero minimum energy in such a medium:

$$E_B=\frac{\hbar^2k_0^2}{2m}, \quad k_0r_s=\operatorname{tg}[k_0(r_s-L)]. \tag{2.30}$$

The Wigner-Seitz approximation should give qualitatively correct results at high liquid densities.

The quantity E_b is an energy barrier for electrons injected from a rarefied gas into a dense medium. Therefore, E_b has been measured in a number of experiments.[91,114,122,123a] The results of E_b measurements in injection of electrons into liquid He at $N=2.2\cdot10^{22}$ cm^{-3} agree fairly well with one another and give $E_b\approx1.2$ eV. This value and others measured at $N>10^{22}$ cm^{-3} show fair agreement with (2.30).[114] It differs sharply from the value 0.67 eV that would be obtained from the optical approximation (2.27). At $N<10^{22}$ cm^{-3} the experimental error[114] becomes greater than the differences between approximations (2.27)–(2.30). These differences decrease in turn with decreasing density.

c) Electron clusters in heavy inert gases

In the preceding sections we have stressed repeatedly that the main cause of the formation of electron and positronium bubbles is the strong exchange repulsion between these particles and atoms of the gas or liquid. However, in addition to short-range repulsion, there is also a long-range attraction. In the case of positronium, it is of a van der Waals nature and has a minor role, and positronium has a positive scattering length on atoms. This points to the possible existence of positronium bubbles in any liquid or gas at sufficiently low temperatures. In the case of the electron, however, the polarization interaction is small only for helium and hydrogen, and only for Ne does it become comparable with the exchange interaction. The scattering length on atoms for heavier inert gases is negative, and the interaction of the electron with these atoms is attractive. Naturally, the existence of bubbles in dense inert gases and liquids is impossible.[28,116] However, bound states between the electron and the medium are possible even in this case.[70] They arise on density bunches, i.e., in clusters, ultimately as a result of the predominance of attractive forces at high polarizabilities.

1) Large-radius clusters. Let us assume that the wavelength of the trapped electron is the largest characteristic length and considerably exceeds the effective radius of the potential $V(r)$. We find that in this case the clusterization condition can be expressed in terms of the amplitude of scattering on this potential. This is important, because the explicit form of the potential $V(r)$ is by no means always well known, whereas experimental information is available on the amplitude of electron scattering on the atom (molecule). Such large-radius clusters can exist in a number of gases, for example in xenon and in dense water vapor.

As usual, the change in free energy has the form

$$\Delta F = K + U + T\Delta S, \tag{2.31}$$

where K is the kinetic energy of the electron and U is its potential energy in the field created by the gas atoms:

$$U=\left\langle\psi\left|\sum_i V(\mathbf{r}-\mathbf{R}_i)-N\bar{V}\right|\psi\right\rangle, \quad \bar{V}=\int V(\mathbf{r})\,d\mathbf{r}. \tag{2.32}$$

The magnitude of the field U depends on the fluctuations of atomic density and R_i is the radius vector of the ith atom. Because of the random distribution of atom coordinates, the probability density of U is of complex form. Let us assume, however, that trapping is most favored at a small deviation of U from its average value. In this case (the random-field approximation), the probability density of U is proportional to $\exp(-U^2/2\overline{U^2})$, where $\sqrt{\overline{U^2}}$ is the variance of the random field. Recognizing that the change in entropy is proportional to the logarithm of the probability, we obtain

$$\Delta F\{\psi, U\}=K+U+\frac{U^2}{2\beta\overline{U^2}},$$

ΔF is a functional of ψ and U. Minimizing it with respect to U, we obtain

$$\Delta F\{\psi\}=K-\tfrac{1}{2}\beta\overline{U^2}. \tag{2.33}$$

The quantity $\overline{V}^2$ will first be analyzed in general form, expressed in terms of the Fourier components of the potential $V(q)$ and the square of the wave function $\varphi(q)$:

$$V(\mathbf{q})=\int V(\mathbf{r})\,e^{i\mathbf{q}\mathbf{r}}\,d\mathbf{r}, \quad \varphi(\mathbf{q})=\int|\psi(\mathbf{r})|^2\,e^{i\mathbf{q}\mathbf{r}}\,d\mathbf{r}.$$

We obtain

$$\overline{U^2}=N\int\left[\int V(\mathbf{r}-\mathbf{r}')\,\psi^2(\mathbf{r}')\,d\mathbf{r}'\right]^2d\mathbf{r}=N(2\pi)^{-3}\int V^2(\mathbf{q})\,\varphi^2(\mathbf{q})\,d\mathbf{q}. \tag{2.34}$$

If trapping is to be possible, it is obviously necessary that the small fluctuation be of sufficient extent and that the electron wave-length λ be large. If it exceeds the effective range of the potential $V(r)$, only the small $q\lesssim\lambda^{-1}$ are essential in (2.34). We further recognize that the effective-radius approximation[18a,2] in the theory of scattering of slow electrons on atoms relates $V(q)$ directly to the scattering amplitude $f(q)$: $V(q)=2\pi\hbar^2m^{-1}f(q)$. This is a result of the fact that the short-range component of $V(r)$ can be described by a delta-shaped pseudopotential, and the Born approximation is applicable to the long-range component. Therefore

$$\overline{U^2}\approx\frac{Nf^2(\lambda^{-1})}{\lambda^3}, \quad \beta\Delta F\approx\frac{\lambda_\beta^3}{\lambda^2}[1-N\lambda_\beta^3\lambda^{-1}f^2(\lambda^{-1})]. \tag{2.35}$$

Thus, $\beta\Delta F$ is expressed in terms of the amplitude of electron scattering on an isolated atom. Since $f(q)$ is well known from experiments, (2.35) can be used for qualitative analysis.

It is easily verified that trapping is possible if the scattering amplitude decreases with increasing electron energy. Figure 15 shows the form of $\Delta F(\lambda)$ qualitatively for $L<0$, i.e., for atoms exhibiting the Ramsauer effect. The increment ΔF increases monotonically at small N/T (curve 1) and trapping is not favored; as N/T increases, ΔF goes negative (curve 2) and passes through a minimum. Stabilization of the clusters is ensured by competition between the short-range and polarization interactions.

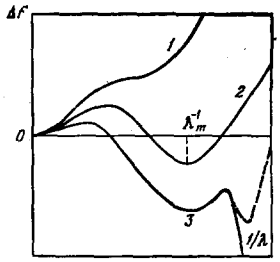

FIG. 15. Qualitative form of free-energy change ΔF vs. electron wavelength λ.

For subsequent analysis we shall use an expression for $f(q)$ in terms of the screening length L and the polarizability α:

$$f(q)=L+\frac{\pi\alpha q}{4a_0}. \tag{2.36}$$

The cross sections obtained from (2.36) for the scattering of electrons on inert-gas atoms agree closely with the experimental values.[18a,2] Substituting (2.36) in (2.35), we obtain $\beta\Delta F$ expressed in terms of the two interaction characteristics L and α. This information on $V(r)$ is sufficient in the long-wave limit. Here we avoid the familiar difficulty that arises in taking account of polarization —the divergence of the potential $\alpha e^2/2r^4$ and the need to cut it off at small r [cf. (1.6)].

The characteristic dimension λ_m of the cluster is easily obtained from the condition for minimum free energy $(\partial F/\partial\lambda=0)$[43,70]:

$$\lambda_m\approx\frac{16\sqrt{\pi\alpha}}{3a_0|L|}\left(1+\sqrt{1-\frac{8\alpha}{3a_0\lambda_\beta^3|L|^3N}}\right). \tag{2.37}$$

The density $N_{cl}(T)$ beginning at which bound electrons predominate over free electrons can be determined from the condition $\Delta F(\lambda_m)=0$:

$$N_{cl}(T)\approx\frac{3\alpha}{|L|^3\lambda_\beta^2a_0}. \tag{2.38}$$

Substituting (2.38) into (2.37), we obtain the value of λ_m^0, which determines the size of the clusters on the transition line $N=N_{cl}(t)$:

$$\lambda_m^0=\frac{4\sqrt{\pi\alpha}}{a_0|L|}. \tag{2.39}$$

At $N=N_{cl}$, the energy binding the electron in the cluster $\varepsilon=\hbar^2/2m(\lambda_m^0)^2$, and the cluster contains one energy level.

Estimates made for Xe in Ref. 43 indicated for the first time that electron clusters may exist in it. Together with the equilibrium phase diagram, Fig. 16 shows a plot of $N_{cl}(T)$ for Xe ($L=-7.1a_0$,[137] $\alpha=27.2a_0^3$). Most of the electrons are trapped at $N>N_{cl}$. Then the sizes of the clusters are around 10–15 Å and they contain about 50 atoms.

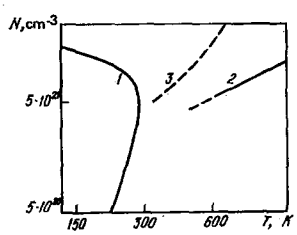

FIG. 16. Value of density N_{cl} at which localization of electrons occurs in Xe (2); gas-liquid phase-coexistence curve (1), and curve corresponding to $NB(T)=1$. $B(T)$ is the second virial coefficient of the interaction between atoms.

The range in which (2.37)–(2.39) are valid on the line $N=N_{cl}(T)$ is determined from the conditions for validity of the Gaussian approximation ($|U|\lesssim\sqrt{\overline{U^2}}$), the long-wave approximation (2.35) ($\lambda\gg|L|, \lambda^2\gg\alpha/a_0$), and the macroscopic cluster-size requirement ($N\lambda^3\gg1$). This gives

$$N_{cl}L^2\lambda_\beta\equiv\xi\gg1,\quad |L|\ll\xi\lambda_\beta,\quad \alpha\ll\xi^2a_0\lambda_\beta^2,\quad N_{cl}\lambda_\beta^3\xi^3\gg1. \tag{2.40}$$

All of these inequalities are easily satisfied in Xe on the segment of the $N=N_{cl}(T)$ curve shown in Fig. 16. The most important one—the first—can be rewritten $l\lesssim\lambda_\beta$, where l is the free path. If the latter is smaller than the wavelength, this indicates trapping according to Mott.[4]

Ways to detect clusters in experiments were proposed in Refs. 43, 70. Observation of a mobility jump at $N\gtrsim N_{cl}$ like the jump observed in dense helium on formation of bubbles would enable us to determine $N_{cl}(T)$.[2)] At $N\gtrsim N_{cl}$, the presence of clusters leads to the appearance of an infrared absorption band in the range in which the gas is perfectly transparent as a result of cluster photoionization. This band lies in the frequency range $\nu\approx\varepsilon/\hbar\approx1500$ cm^{-1}, and its measurement makes it possible to determine the electron binding energy in the cluster. At $N>N_{cl}$, the injected electrons have very low mobility. Irradiation of the gas with a light source of frequency of the order of ν results in photoionization and a sharp mobility jump. This experiment, which was performed in liquid He^4,[91] made it possible to determine the electron binding energy in a bubble. A similar experiment can be designed to determine the properties of clusters.

Large-radius electron clusters can also exist in other gases, including molecular ones. For example, in neopentane ($C(CH_3)_4$), whose molecules are symmetric and possess high polarizability, the existence region of clusters is similar to that found for Xe. Below we shall discuss the possibility of cluster formation in gases of dipolar molecules. On the other hand, in gases whose atoms possess low polarizability (for example, Ar and methane CH_4), formation of clusters is not favored even though the scattering length is negative.

2) Small-radius fluctuons. Small-radius complexes may exist in dense gases in addition to large-radius clusters. The tendency to their formation can be traced in Fig. 15. As λ increases, the ΔF curve undergoes a new, qualitative change (curve 3, which corresponds to large N/T), passing through a second maximum and even decreasing without limit. However, allowance for the repulsion of atoms within the fluctuon may stabilize the complex, as indicated by the dashed curve in Fig. 15. Then small-radius complexes will exist side-by-side with large clusters, with their concentra-

[2)] A substantial decrease in electron mobility was recently[123b] observed near the "gas-liquid" phase coexistence curve in measurements of electron drift velocities in dense gaseous xenon; this apparently indicates self-trapping of electrons with formation of clusters.

tions related as $\exp[-\beta(\Delta F_s - \Delta F_i)]$, where ΔF_s and ΔF_i are the values of ΔF at the corresponding minima of the $\Delta F(\lambda)$ curve.

Many of the electrons are localized in small-radius complexes at low temperatures in the state of thermodynamic equilibrium.[43] Also at low temperatures, however, fluctuons are produced on small Gaussian fluctuations of large radius (see Chap. 2, Sec. b), and this initially results in the formation of large-radius clusters. They are separated by an energy barrier from the small-radius complexes and may have rather long lifetimes. In actual experiments, these times may be found comparable to the characteristic time of the measurements. In that case, the small-radius complexes will not be observed.

The properties of small-radius fluctuons differ significantly from the properties of large clusters. The simplest way to verify this is to refer to the square-well model. Let us assume that it is possible for an electron to be trapped in a spherical fluctuon of radius R with rectangular walls, the density N_1 of the atoms within which differs from the average N by an amount ΔN ($N_1 = N + \Delta N$). Normally, the field acting on the electron in a fluctuon is assumed equal to $2\pi\hbar^2 L\Delta N/m$. In the case of high polarizability α of the atoms, however, it is necessary to remember that the scattering length L is an integral characteristic of potential $V(r)$, and that all distances out to infinity contribute to it. On the other hand, the wave function of the trapped electron decreases exponentially at distances greater than R. Thus, we must exclude the contribution to L from distances $r > R$. This is equivalent to introducing an additional field equal to $4\pi\Delta N\int_R^\infty V(r)r^2dr = 2\pi\alpha e^2\Delta N/R$. Then, assuming that the potential well is sufficiently deep, we can write for the binding energy ε of the electron in the fluctuon

$$\varepsilon(R) = -\frac{2\pi\hbar^2 L\Delta N}{m} - \frac{2\pi\alpha e^2\Delta N}{R} - \frac{\pi^2\hbar^2}{2mR^2}.$$

As usual, the change in free energy as a result of electron trapping in the fluctuon $\Delta F = -\varepsilon + T\Delta S$, where $\Delta S(R) = (4\pi/3)R^3[N_1 \times \ln(N_1/N) - \Delta N]$. The concentration of the atoms within the fluctuon can be found from the minimum condition:

$$N_1(R) = N\exp\left[-\frac{3\lambda_\beta^3}{R^3}\left(L + \frac{\alpha}{a_0 R}\right)\right]. \qquad (2.41)$$

It follows from (2.41) that large-radius ($R > |L|a_0/\alpha$) fluctuons are clusters ($N_1 > N$) if $L < 0$, while small-radius fluctuons ($R < |L|a_0/\alpha$) are more likely to be bubbles ($N_1 < N$). Mixed-type formations—cavities surrounded by bunches of atoms—apparently exist in the intermediate range. The cavity is formed as a result of short-range exchange repulsion between the electron and the atoms, and the bunching by polarization attraction.

In the case of small clusters, the optimum size R_n and the $N_{cl}(T)$ are given by expressions that agree with (2.37) and (2.38) within a constant. On the line of transition to trapped states $N_{cl}(T)$

$$N_1(R_{cl}) = N\exp\left(\frac{2}{27}\frac{\lambda_\beta^3 L^4 a_0^3}{\alpha^3}\right). \qquad (2.42)$$

Relation (2.42) indicates that $N_1 \simeq N$ at high temperatures, the Gaussian approximation is valid, and the interaction among the atoms in the cluster can be neglected. N_1 increases with decreasing temperature, and it becomes important to take this interaction into account. Naturally, allowance for the interatomic repulsion is mandatory for small-radius fluctuons.

The role of interatomic repulsion can be traced most simply with the aid of the lattice-gas approximation, remaining within the framework of the square-well model. In this case, the entropy change [see (2.23)]

$$\Delta S(R) = \frac{4\pi}{3}R^3\left(N_1\ln\frac{N_1}{N} - \frac{1-N_1 b}{b}\ln\frac{1-N_1 b}{1-Nb}\right). \qquad (2.43)$$

Minimizing ΔF with respect to N_1, we obtain instead of (2.41)

$$N_1(R) = \frac{N\exp(-3\lambda_\beta^3 L^*/R^3)}{1-Nb\,[1-\exp(-3\lambda_\beta^3 L^*/R^3)]}, \quad L^* = L + \frac{\alpha}{a_0 R}, \qquad (2.44)$$

and $\Delta F(R)$ takes the form

$$\beta\Delta F = \frac{\pi^2\lambda_\beta^3}{R^2} - 4\pi N\lambda_\beta^3 L^* + \frac{4\pi}{3}\frac{R^3}{b}\ln\left\{1 - Nb\left[1 - \exp\left(-\frac{3\lambda_\beta^3 L^*}{R^3}\right)\right]\right\} \qquad (2.45)$$

at high densities $(Nb \to 1)\beta\Delta F \approx \pi^2\lambda_\beta^2/R^2$, i.e., allowance for repulsion does indeed result in the appearance of a second minimum of $\Delta F(R)$ and eliminate its nonphysical behavior at small R. The conditions under which small-radius clusters are formed and their properties can be determined from the conditions $\partial\Delta F/\partial R$ and $\Delta F = 0$. The resulting expressions are quite cumbersome and will not be printed here.

3) Correct account of polarization and interatomic interaction. Comparison with experiment. The simple model presented in the preceding section indicates the importance of considering the polarization interaction and predicts the existence of new quasiparticles—clusters. However, the results obtained are only qualitative because of the assumptions made. The self-consistent-field method was used in Ref. 43 to take correct account of polarization interaction in the case of fluctuations of arbitrary depth and shape, and not only the repulsion, but also the attraction between atoms of the gas was considered. Applied to light inert gases, this made is possible to establish the influence of polarization interaction on the properties of bubbles in He and H_2.

In the self-consistent-field method, the change in system free energy as a result of electron trapping, with formation of either a bubble or a cluster, is determined by expression (2.7), in which the effective potential $V(\mathbf{r})$ equals

$$\tilde{V}(\mathbf{r}) = \int V(\mathbf{r}-\mathbf{r}')|\psi(\mathbf{r}')|^2 d\mathbf{r}'. \qquad (2.46)$$

It has been shown[43] that if the electron wavelength λ in the cluster or bubble is sufficiently large, i.e., if

$$\lambda^2 \gg \frac{\alpha}{a_0}, \quad \lambda \gg |L|,$$

$\tilde{V}(r)$ can be written in the form

$$\tilde{V}(r) = 4\pi\frac{\hbar^2 L}{2m}|\psi(\mathbf{r})|^2 - \frac{\alpha e^2}{2}\int\frac{|\psi(\mathbf{r}')|^2 - |\psi(\mathbf{r})|^2}{(\mathbf{r}-\mathbf{r}')^4}d\mathbf{r}'. \qquad (2.47)$$

We observe that this expression does not contain divergences as $r \to 0$, and that all information on the

interaction potential is present in well-known characteristics—the scattering length L and the polarizability α. This is directly related to the theory of scattering of slow electrons on atoms,[18a,2] which expresses the scattering amplitude only in terms of L and α.

In Ref. 43, the interatomic interaction was taken into account in the pair approximation in the lattice-gas model.[6] The calculation was made with the trial wave function (2.10). Figure 17 presents the results of numerical calculation of $\Delta F(\lambda)$ in Xe for three values of T and densities such that $\Delta F_l = 0$, i.e., when the number of free electrons was equal to number of electrons trapped in large-radius clusters. Figure 17 indicates that there are no small-radius clusters at high temperatures (curve 1). As the temperature declines, they appear, and may even come to predominate (curve 3). Calculated results for $\tilde{N}_{cl}(T)$ in Xe appear in Fig. 18.

In gases in which the electron is for the most part repelled from atoms ($L>0$), allowance for polarizability may also produce significant corrections. Figure 18 shows $N_{cl}(T)$ curves plotted for He^4 and H_2 with and without allowance for the polarization interaction. We see that allowance for this interaction lowers N_{cl}, and by larger amounts the higher the temperature. The correction due to this effect is small in He because α is small. In H_2, allowance for the polarization interaction lowers N_{cl} by 20–50%. Figure 18 also shows values obtained for N_{cl} in electron-mobility experiments in He^4.[23]

It is clearly seen from Fig. 18 that the $N_{cl}(T)$ relations for He^4 and H_2 are qualitatively different from the relation in Xe. Actually, according to (2.5), we have $N_{cl} \sim T^{2/3}$ in the case of bubbles, while (2.38) gives $N_{cl} \sim T$ for clusters.

4) Orientation clusters in a gas of dipolar molecules. In a medium of polar molecules, trapping may be due not so much to density bunching (or rarefaction) around the charge as to preferential orientation of the dipoles to the charge. This results from the lack of central symmetry of the electron-molecule interaction potential:

$$V(\mathbf{r}) = -\frac{(\mathbf{d}\cdot\mathbf{r})}{r^3}, \tag{2.48}$$

where $\mathbf{d}$ is the dipole moment of the molecule. Such

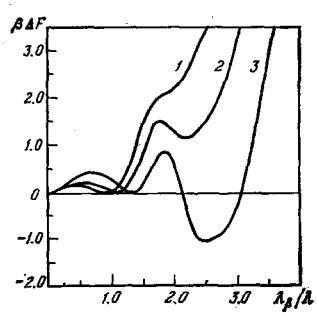

FIG. 17. Plots of $\beta\Delta F$ against λ_β/λ in Xe.[43] Curves for which $\Delta F_l = 0$ are shown: 1) $T = 700$ K, $N = 2.5 \cdot 10^{21}$ cm^{-3}; 2) $T = 600$ K, $N = 1.9 \cdot 10^{21}$ cm^{-3}; 3) $t = 500$ K, $N = 1.3 \cdot 10^{21}$ cm^{-3}.

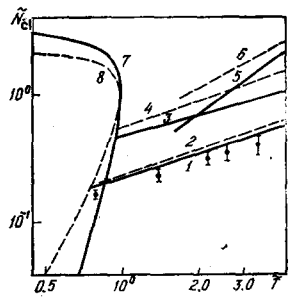

FIG. 18. Value of reduced density $\tilde{N}_{cl}(\tilde{T}) = N_{cl}(T)/\tilde{N}_c$ at which electron trapping occurs[69]; curves 1–6. Curves 1 and 2 for He^4 and curves 3 and 4 for H_2 (curves 2 and 4 do not take account of the polarization interaction); curves 5 and 6 for Xe (curve 6 is the Gaussian approximation with the interaction between atoms); 7, 8) phase-coexistence curves in Xe and He^4, respectively. The symbols are experimental values of N_{cl} in He^4 (Ref. 23) ($\tilde{T} = T/T_c$).

an orientation cluster is similar to the hydrated or solvent-separated electron, both of which have been thoroughly studied in experiment and theoretically.[124-126] However, the conditions in a gas differ favorably from those in polar liquids. A whole series of difficulties that are basically associated in liquids with the allowance for the short-range component of the potential $V(\mathbf{r})$ disappears in the more rarefied system. In the absence of experimental data, this enables us to indicate the range in which such states may exist.[127]

By analogy with the problem of electron state in strongly polarized gases, we may assume that the electron can be trapped in the case of small deviations of the interaction energy from the average. It is then possible to use formula (2.23) to calculate ΔF, introducing the structure factor $S(\mathbf{k})$ to take account of the interaction among gas molecules. Then

$$\Delta F\{\psi\} = \frac{\hbar^2}{2m}\int \mathbf{k}^2\psi^2(\mathbf{k})\frac{d\mathbf{k}}{(2\pi)^3} - \frac{1}{2}\beta N\int |\tilde{V}(\mathbf{k})|^2 S(\mathbf{k})\frac{d\mathbf{k}}{(2\pi)^3}, \tag{2.49}$$

$$S(\mathbf{k}) = 1 + N\int e^{-i\mathbf{k}\cdot\mathbf{R}}[g(\mathbf{R})-1]\,d\mathbf{R} + N\int [g(\mathbf{R})-1]\,d\mathbf{R}, \tag{2.50}$$

where $g(R)$ is the binary correlation function of the molecules. The interaction among the molecules that compose the excess density over the average [second term in (2.50)] and the interaction between them and the homogeneous background (third term) contribute to ΔF. The explicit dependence of S on $\mathbf{k}$ is determined by the inhomogeneity of the medium that results from clusterization.

The intermolecular interaction in a moderately dense gas can be described in the pair approximation. The intermolecular potential $u(\mathbf{R})$ has a short-range repulsive isotropic component and a long-range dipole-dipole component

$$u_L(\mathbf{R}) = \frac{(\mathbf{d}_1\cdot\mathbf{d}_2) - 3(\mathbf{d}_1\cdot\mathbf{R})(\mathbf{d}_2\cdot\mathbf{R})R^{-2}}{R^3}. \tag{2.51}$$

Since $u_L(\mathbf{R})$ depends on the mutual orientation of the dipoles $\mathbf{d}_1$ and $\mathbf{d}_2$, ΔF must be averaged over it, and this will be done below. The interaction (2.51) is attractive in a homogeneous gas and repulsive in an

oriented-dipole medium.[126]

We shall confine ourselves to the case of high temperatures, in which $\beta|u_L(R)| \ll 1$. The structure factor then has the form

$$S(\mathbf{k}) \approx 1 - 2Nb - \beta u_L(\mathbf{k}) - 2NB(T),$$

where $u_L(\mathbf{k}) = 4\pi(k\cdot d_1)(k\cdot d_2)/k^2$ is the Fourier transform of (2.51), b is the quadrupled intrinsic "volume" of the molecule, and $B(T)$ is the second virial coefficient.

In the adiabatic approximation, in which the characteristic electronic times are much smaller than the times of spatial displacement and the times of reorientation of the dipoles in the localization region, the wave function $\psi(\mathbf{r})$ must be spherically symmetric. In this case, $\tilde{V}(\mathbf{R})$ equals

$$\tilde{V}(\mathbf{R}) = -\cos(\mathbf{d}\cdot\mathbf{R})\frac{ed}{R^2}\int_0^R |\psi(r)|^2\cdot 4\pi r^2\,dr. \qquad (2.52)$$

We find the minimum of $\Delta F\{\psi\}$ by the variational method, using the trial function (2.15). We obtain

$$\Delta F\{\psi\} = \Delta F(\lambda) = \frac{3}{4}\lambda^{-2} - \frac{4\sqrt{2\pi}}{3}Nd^2\lambda_\beta^3\lambda^{-4}\left(1 - 2Nb - 2NB - \frac{4\pi Nd^2\beta}{3}\right); \qquad (2.53)$$

here and below all quantities are expressed in atomic units. Variation with respect to λ gives

$$\beta\Delta F(\lambda_0) = -\frac{3}{2}\left(\frac{\lambda_\beta}{\lambda_0}\right)^2,$$
$$\lambda_0^{-1} = \frac{8\sqrt{2\pi}}{9}N\lambda_\beta^3 d^2\left(1 - 2NB - 2Nb - \frac{4\pi}{3}Nd^2\beta\right), \qquad (2.54)$$

where λ_0 is the wavelength of the trapped electron. The intermolecular interaction increases the size of the cluster, preventing it from forming. In the first approximation, however, $\lambda_0^{-1} = N\lambda_\beta^2 d^2$. This makes it possible to rewrite the condition for dominance of trapped over free states, $\beta|\Delta F(\lambda_0)| \gtrsim 1$, in a different form:

$$Nq\lambda_\beta \gg 1, \quad q = \frac{8\pi\lambda_\beta^2 d^2}{3}. \qquad (2.55)$$

The criterion (2.55) is analogous to (2.40) and q is the Born cross section for scattering of the electron on the dipole.

The distribution of the excess molecules in the cluster, $n(\mathbf{R}, \Omega)$, over the coordinates R and the orientations (Ω is the angle between d and R) is given by Boltzmann's formula

$$n(\mathbf{R}, \Omega) = N(e^{-\beta\tilde{V}(\mathbf{R})} - 1). \qquad (2.56)$$

It is essential that $n(\mathbf{R}, \Omega) = -\beta NV(\mathbf{R})$ in the present approximation. Therefore bunching around the electron does not occur and $n(R) = \int n(\mathbf{R}, \Omega)\,d\Omega/4\pi = 0$. The states are purely orientational. They are similar to large-radius polarons. Unlike the polaron, however, the self-trapped state of an electron in a disordered medium is localized almost in the literal sense, since the mobility of this massive particle is extremely low.

We recall that the expressions derived above are valid if $\beta|\tilde{V}(\mathbf{R})| \ll 1$ [the depth (2.52) is proportional to $d\cos(\mathbf{d}\cdot\mathbf{R})/\lambda^2$] and $N\lambda_0^3 \gg 1$. These inequalities are compatible with (2.55) if

$$N\lambda_\beta^3 d^2 \gg 1, \quad d \ll 1. \qquad (2.57)$$

Naturally, the range of validity is limited to small dipole moments d. This would appear to prohibit application of the theory to water vapor, since it has $d = 0.725$, i.e., not small. But the literal inequalities (2.57) contain small numerical multipliers. This enables us our expressions to indicate the limit of trapping $N_{cl}(T)$ on a density-temperature diagram. Curve 2 in Fig. 19 is that of $N_{cl}(T)$. At $T = 1000$ K on curve 2, the clusters contain a large number of molecules $(4\pi/3)Nr_0^3 \approx 50$, where r_0 is the cluster "radius" determined from the condition $(4\pi/3)r_0^3|\psi(0)|^2 = 1$. Mutual repulsion of the dipoles results in a steeper $N_{cl}(T)$ curve.

Trapped states of electrons in water were found in Ref. 128a. The liquid range was investigated most thoroughly, but measurements were also made at $T > T_c$ up to $T = 390$ C at $\rho \approx \rho_c$. The absorption spectrum of water was measured as electrons were injected into it. As in studies of liquid helium at supercritical temperatures, there was an absorption band corresponding to transition of the electron from the fluctuon ground state to the continuous spectrum. The absorption maximum was observed at a light-quantum energy of ≈ 1 eV. As Fig. 19 shows, the density level ρ_c is quite far from the clusterization curve 2. Therefore the approximation of small extended fluctuations becomes invalid. On the other hand, we should expect dense clusters around the electron. Such states were discussed in Ref. 128b, the results of which agree well with the experimental data of Refs. 128a and b. Absorption-spectrum measurements were made on the saturated-vapor line in Ref. 128c.

d) Positron clusters. Critical point of clusterization phenomenon

Unusual behavior of the positron annihilation rate λ_1 has been observed[71,72] in experiments on the annihilation of positrons in dense gaseous He^4 at low temperatures. At high temperatures, λ_1 is independent of T as usual and proportional to the density N of the gas (see below, Fig. 20). At a certain "critical" temperature T_{cl}, λ_1 increases jumpwise and reaches the values characteristic for liquid He^4. It is natural to attribute this increase in annihilation rate to an increase in the density of the atoms around the positron—as a result of either chemical bonding or polarization of the medium and formation of positron clusters analogous to the electron clusters discussed in the preceding section.

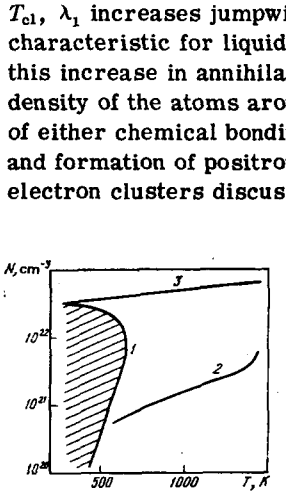

FIG. 19. Density-temperature diagram of water. 1, 3) phase equilibrium curves; curve 2 represents $N_{cl}(T)$.

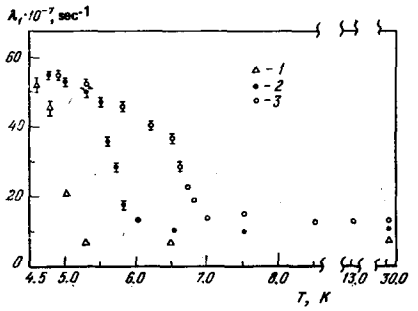

FIG. 20. Positron annihilation rate in gaseous He^4. Densities (g/cm^3): 0.016 (1), 0.023 (2), and 0.030 (3).

This analogy becomes more obvious when it is remembered that the scattering length of positrons on atoms is negative, i.e., as in the case of electrons, attractive forces predominate in heavy inert gases.

Bound states of the positron with He^4 atoms in the ground state apparently do not exist.[129] Another possibility has been discussed.[46] Working essentially from Atkins's model,[130] which is valid for heavy classical ions, Canter *et al.*[46] made estimates that did not confirm the possibility of cluster formation in He^4. Thus the question as to the nature of clusters in both helium and argon[106] remained open. The possibility of positron-cluster formation in dense gases was affirmed in Ref. 73. Here the existence region of the clusters was found to be limited not only at the low-density end but also at high densities, and to be adjacent to the "gas-liquid" phase coexistence curve on the higher-temperature side. This made it possible to predict the existence of a "critical" temperature for the positron clusterization effect, above which clusters are absent. "Critical" clusterization points were recently observed in He^4 and He^3.[74a]

1) Positron clusters and annihilation of slow positrons. All of the basic effects that can be observed in a change in the annihilation rate of slow positrons follow from a simple model:

1) the interaction of e^+ with the atom is described by a Fermi pseudopotential with a scattering length L (1.3);

2) the lattice-gas approximation is used for the entropy change ΔS with allowance for both interatomic repulsion and attraction;

3) e^+ is localized in a spherical volume of radius R that is uniformly filled by atoms at the highest possible density $1/b$.

For this model

$$\beta\Delta F = \pi^2\lambda_\beta^2 R^{-2} + 4\pi L\lambda_\beta^2\Delta N + \frac{4\pi}{3}R^3\left[b^{-1}\ln\frac{1}{1-\Delta Nb} - a(\Delta N)^2\right]. \quad (2.58)$$

The first term in (2.58) is the kinetic energy of e^+, the second is the potential energy, $\Delta N = b^{-1} - N$ is the excess density of the atoms in the cluster, $a = T_c/N_c$, and $b = 1/2N_c$.

The region in which a large fraction of the positrons is localized is bounded by the $N_{cl}(T_{cl})$ curve determined by the equation system $\Delta F = 0$, $\partial\Delta F/\partial R = 0$. Solving it, we obtain $N_{cl}(T_{cl})$ (or $T_{cl}(N_{cl})$) and the optimum-cluster size R_{cl}:

$$\frac{T_{cl}}{T_c} = -\frac{(1-N_{cl}b)^2}{\ln N_{cl}b}\left[\frac{a}{bT_c} + c\frac{|L|^{5/2}\lambda_c^2}{b^{3/2}}\sqrt{1-N_{cl}b}\right], \quad (2.59)$$

$$R_{cl} = \sqrt{\frac{5\pi}{12|L|}\left(\frac{1}{b} - N_{cl}\right)^{-1}}, \quad (2.60)$$

where $c = 16(3/5)^{5/2}\pi^{-3/2}$, $\lambda_c = \hbar/\sqrt{2mT_c}$. The existence region of the clusters is naturally bounded both on the side of low N and on the high-N side, since the compressibility of the matter is limited. This also follows from formula (2.59), which has two roots N_{cl} at low temperatures. These two values of N_{cl} move together as the temperature rises and are finally equal at $T_{cl} = T^*$. Equation (2.59) has no solutions at temperatures above T^* at any N, i.e., formation of clusters is thermodynamically unfavorable at $T > T^*$.

Thus, the existence region of the clusters, which is bounded by the $N_{cl}(T_{cl})$ curve, borders on the two-phase region of the gas, having a "critical" temperature $T^* > T_c$. We may write with sufficient accuracy

$$\frac{T^*}{T_c} \approx 0.41\left(\frac{a}{bT_c} + 0.85|L|^{5/2}\lambda_c^2 b^{-3/2}\right), \quad N^* \approx 0.28\, b^{-1}. \quad (2.61)$$

The results obtained here are valid only for extended clusters, which must contain a large number of atoms and have densities close to the close-packed value. This implies satisfaction of the inequalities

$$|L| \ll R, \left(\frac{4\pi}{3}\right)R^3\frac{1}{b} \gg 1, \quad 1 - Nb \ll Nb\exp\left(\frac{3L\lambda_\beta^2}{R^3} + Nb - 1\right). \quad (2.62)$$

Let us make estimates for Ar and Ne. We assume $L_{Ar} = -3.5a_0$ (according to Ref. 131, $-3 \geq L_{Ar} \geq -4a_0$) and $L_{Ne} = -0.6a_0$.[132] For Ar we obtain $T^* \approx 1.6T_c$, i.e., there is a rather broad existence region of clusters. This is consistent with the experiment of Ref. 106, where a sharp increase in the annihilation rate of e^+ in Ar was observed under certain conditions. In Ne, T^* is practically equal to T_c and, consequently, clusters can exist only in a very narrow region. In fact, no anomalies of the annihilation rate in Ne were observed in Ref. 106.

Figure 20 shows a plot of $\lambda_1(T)$ in He^4 as measured in Refs. 72 and 46 at three different densities. We see that λ_1 is practically independent of N and T at low temperatures and has values λ_L that are characteristic for liquid He^4 (in liquid He^4 at the saturation vapor pressure, for example, $\lambda_1 \approx 5.0 \cdot 10^8$ sec^{-1} at 4.2 K and $5.5 \cdot 10^{-8}$ sec^{-1} at the λ-point[46]). At high temperatures, $\lambda_1 \ll \lambda_L$, it is independent of T and proportional to N, and has values λ_G that all characteristic for all gases at high temperatures [see formula (1.15)]. It is natural to determine the temperature T_{cl} from the condition that the positron can, with equal probability, be either free or localized at the given density N and $T = T_{cl}$ ($\lambda_1(T,N)|_{T=T_{cl}} = [\lambda_G(N) + \lambda_L]/2$). The $T_{cl}(N)$ values obtained in this way appear in Fig. 21. Also included are values of $T_{cl}(N)$ for Ar that were obtained by similar reduction of the experimental data from Ref. 106.

Numerical calculations were made in Ref. 73 by the self-consistent-field method for quantitative comparison with experiment, much as in the case of electron

clusters (see the preceding section and Ref. 43). The interaction between the atoms in the cluster was taken into account within the framework of a van der Waals model with constants a and b obtained by reduction of the empirical equation of state in the appropriate density and temperature ranges. The calculated results for He^4 and Ar appear in Fig. 21. A large fraction of the positrons is localized inside the $N_{cl}(T)$ curves, and the annihilation rate approaches the liquid rate λ_L. The plotted N_{cl} points obtained in Refs. 46 and 106 correspond to the low-temperature part of the lower branch of the $N_{cl}(T)$ curve. It was shown in Ref. 73 that the range of variation of the parameters must be broadened, especially in temperature, to determine the critical clusterization point. This was done in a recent study (Ref. 74a), which will be discussed below.

The curves in the figure show that the formation of clusters is not favored over almost the entire upper branch of the gas-liquid phase-coexistence curve (i.e., in the liquid), but that they can exist near the actual critical point. This quite consistent with the recently observed sharp increase of λ_1 in liquid He^3 at $T = 3.05$ K, i.e., near T_c,[133] which attests to transition of the positrons to a trapped state. As for the liquid, no anomalies in the variation of λ_1 were observed far from T_c.

Let us indicate certain characteristics of positron clusters. At $T = 7$ K in He^4, they have a size $\sim 25a_0$, consistent of ~300 atoms, and have a binding energy of ~0.1 eV. The density in the cluster is around $2.5N_c$, i.e., it corresponds to the density of the liquid.

2) Critical point of clusterization. The transition of positrons (electrons, positronium) from the free to the trapped state takes place abruptly, in a narrow temperature range, and can be treated as a smeared second-order phase transition in the positron subsystem. On the other hand, a thermodynamically stable region of elevated (lowered) density forms around the light particle on formation of clusters (bubbles) and can be treated as a new-phase zone. This makes the transition initiated by the light particles similar to an ordinary gas-liquid phase transition, except that it occurs in microscopic volumes. This analogy is most conspicuous in the case of positron clusters, where the shape of the $N_{cl}(T)$ curve, which bounds the region of cluster existence, is very similar to that of the gas-liquid coexistence curve, and both of them have a critical point.

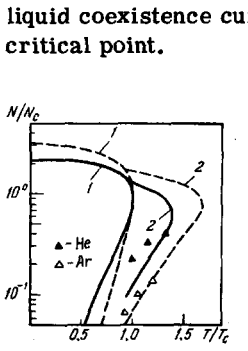

FIG. 21. Phase-coexistence curves (1) and clusterization curves $N_{cl}(T)$ (2). The solid curves are for He^4, the dashed curves for Ar, and the symbols represent experiment.[46,106]

The upper branch of the $N_{cl}(T)$ curve results from the fact that the interatomic interaction increases with increasing density. Here the compressibility of the gas drops sharply and the work that must be done to create a fluctuation increases. Trapping becomes thermodynamically unfavorable. These arguments apply not only to clusters, but also to bubbles, for which a similar $N_{cl}(T)$ branch and critical point could exist in principle. However, there is a qualitative difference between bubbles and clusters: the density of the atoms is low within a bubble and the compressibility of the gas is always near unity (even if the average density of the gas is high and its compressibility $\ll 1$), while in clusters the density of the atoms is always higher than the average, and, accordingly, the compressibility is below-average. Therefore even if an upper $N_{cl}(T)$ branch does exist for bubbles, it lies much higher than the corresponding branch for clusters. Quantitative estimates made in Ref. 28 indicated that the formation of electron bubbles in He^4 is thermodynamically favored all the way up the melting point and, consequently, that the upper $N_{cl}(T)$ branch may lie exclusively in the solid phase.

The existence region of positron clusters in He^4 and He^3 was determined experimentally in Ref. 74a. As in Refs. 46, 72, and 106, the positron annihilation rate was measured as a function of density at various temperatures, but the range of variation of the parameters was broadened considerably for both density and temperature.

The $N_{cl}(T)$ curve bounding the cluster existence region in Ref. 74a agrees qualitatively with the region proposed by Khrapak and Yakubov[73] and confirms their prediction of a critical temperature T^*. The measured parameters of the critical point for the microscopic phase transition (He^4: $T^* = 8.4$ K, $N^* = 10^{22}$ cm^{-3}; He^3: $T^* = 6.6$ K, $N^* = 9 \cdot 10^{21}$ cm^{-3}) also agree fairly well with theory.[73] The positron-clustering phenomenon was analyzed in Refs. 74b and c within the framework of the model proposed in Ref. 73. Among other things, the known values of the trapped-positron wave function and formulas similar to (2.17) and (2.18) were used to compute the positron annihilation rate λ_1. The results of the calculation[74b] for He^4 appear in Fig. 22b. They agree well with experiment, which is represented in Fig. 22a.

The information obtained in Ref. 74a on the properties of the clusters themselves is consistent with the

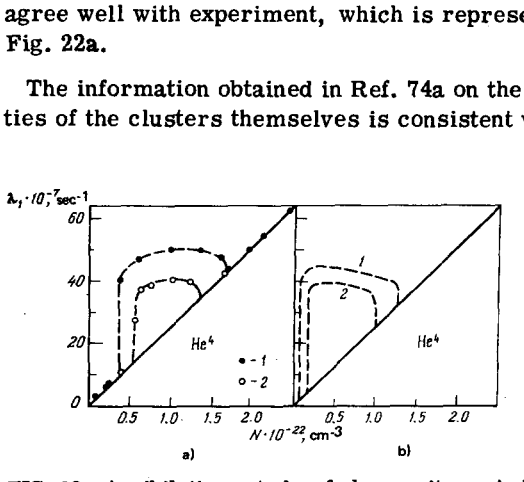

FIG. 22. Annihilation rate λ_1 of slow positrons in He^4. a) experiment[74a,b]; b) theory.[74b]

estimates of Ref. 73. Thus, the dimension of the clusters was found equal to 10–20 Å, while the density of the atoms in the cluster was 2–3 times the critical density N_c of the gas.

According to (2.61), a rising sequence of T^*/T_c should be observed in other inert gases. It is smallest in Ne and, accordingly, no anomalies in the annihilation rate have been detected in Ne.[106] The ratio T^*/T_c can be measured in Ar if the temperature variation range of Ref. 106 is broadened. The values of T^*/T_c should be larger for heavy inert gases (Kr, Xe) than in the case of Ar.

The electron clustering region should also be bounded in temperature. This also pertains to clusters in Xe [Chap. 2, Sec. c)]. The ratio T^*/T_c is somewhere in the region of 1000 K. A critical point may also exist for fluctuons in dense water vapor.

3. CERTAIN APPLICATIONS

The phenomena considered above are interesting not only for experimental physics, but also for many specific applications. Most of them make use of the properties of the system in external fields. Here, problems of kinetics in dense systems that have not yet been solved often press into the foreground. Let us discuss some of the applications in order to stress this once again and identify unsolved problems.

a) The Townsend ionization coefficient

Electrons injected into a cold gas may, in an external electric field f, acquire energy sufficient to ionize atoms of the gas with which they collide. The result is an electron avalanche, i.e., the number of electrons increases exponentially. The argument of the exponential contains a quantity α, which is known as the first Townsend ionization coefficient:

$$\alpha = \frac{\nu_i}{W}, \tag{3.1}$$

where ν_i is the average frequency of ionization and W is the drift velocity. It is known that the value of $\eta = \alpha/F$ depends only on the ratio F/N for a given gas.[134]

The quantity α is of prime importance for a number of phenomena involving the development of ionization, e.g., for the sparkover phenomenon. The values of α for rarefied gases are well known. Interest in very high densities has recently been stimulated by the problem of creating counters that work in condensed media. Figure 23 presents early experimental data obtained in liquid Xe.[135] They demonstrate the radical departure from the universal curve 1 obtained in rarefied gas.

Let us discuss the density effects that influence the Townsend coefficient.[136] To determine the energy ε of the electrons in the field F, we write their energy balance, equating the elastic losses to the Joulean heat:

$$\delta \varepsilon \nu = eFW. \tag{3.2}$$

The notation of Chap. 1 has been used here. The structure factor (1.14) may differ considerably from

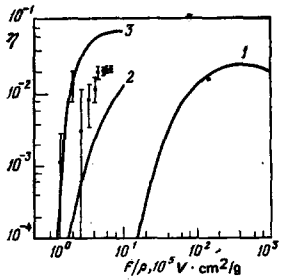

FIG. 23. Plots of η against F/ρ. The symbols represent measurements in Xe at density $\rho = 3.06$ g/cm^3 and $T = 163$ K.[135] Curve 1 represents experiment in rarefied gas, curves 2 and 3 the calculation made in Ref. 136.

unity in dense matter and must be taken into account in writing the drift velocity $W = eF/m\nu S(0)$.[41] Recognizing that the cross section q for scattering of an electron on an Xe atom increases with the electron's energy as $\varepsilon^{3/2}$,[137] we find from (3.1) that $\varepsilon \sim (F^2/N^2 S(0))^{1/5}$. Since ε is of electron-volt order, the implicit assumptions are satisfied. First, the nonpairing effects on scattering are small [see Chap. 1, Sec. b)]. Second, all electrons were assued to be free, since the high kinetic-energy values prevent trapping (see Chap. 2).

We next draw attention to the fact that the sharp dependence of η on F/N (Fig. 23) is due chiefly to the exponential dependence of η on E_1/ε, where E_1 is the ionization energy (the other relationships are power-law). The second density effect is governed by the decrease in E_1 that results from the boundary shift of the continuous spectrum:

$$\Delta E_1 = E_1 - E_1(N) = -\frac{2\pi\hbar LN}{m} + \alpha e^2 N \int g(\mathbf{r}) \frac{1}{2r^4} d\mathbf{r}. \tag{3.3}$$

This shift is governed by the electron-atom interaction [written in the optical approximation (2.27)] and by the ion-atom interaction. Under certain conditions, the ground-state shift must also be taken into account.[138] Thus, η depends exponentially on $E_1(N)[N\sqrt{S(0)}/F]^{2/5}$, while in the rarefied gas it depended on $E_1(N/F)^{2/5}$. As a result, η becomes the function

$$\eta = \eta\left(\frac{F}{N\sqrt{S(0)}}\left[\frac{E_1}{E_1(N)}\right]^{5/2}\right)$$

in matter—the same function that we have for the rarefied gas, $\eta = (F/N)$.[136]

The result obtained makes it possible to use the $\eta(F/N)$ relation (curve 1), shifting it along the axis of abscissas in accordance with the values of $S(0)$ and $E_1(N)/E_1$. This results in curve 2, which describes the results of the measurements qualitatively.

The actual situation is more complex. The interaction not only shifts the boundary of the continuous spectrum, but also strongly modifies the spectrum of electronic states. This raises the question of ionization and excitation kinetics in the dense system. The only thing that can be said at present is that the excitation losses of electron energy in the liquid (with subsequent deexcitation) are sharply reduced. In fact, the discrete spectrum has only one (or two) weakly bound levels of the exciton type. Curve 3 in Fig. 23 was plotted without considering any losses at all, thereby bounding η from above. The nature of the excitation

and ionization kinetics in the dense gas remains unclear.

b) Corona discharge in cryogenic helium

Much attention is currently being given to the dielectric strengths of liquid and dense gaseous helium in connection with the development of high-voltage superconductive systems (cables, magnets).[139,140] The high dielectric strength of helium in homogeneous electric fields[139,141] indicates that it might be used not only as a refrigerant, but also as a good insulator. Study of the electrical discharge under conditions of a strongly inhomogeneous field, for example a corona discharge,[142] is important for specification of optimum working conditions for specific systems. This is because sparkover may be initiated at microscopic projections on the surface of the electrodes, with appearance of a local corona, at high electric-field strengths. Initiation of the corona discharge is responsible on the one hand for the bulk of the energy losses in the line (cable) at subsparkover voltages. Theoretical study of the corona discharge and sparkover in cryogenic helium encounters major difficulties owing to lack of the necessary information on the kinetics of ionization in dense gases, on the kinetics of trapping, and on the spatial distribution of the charge (when either free or trapped electrons diffuse) and a whole series of nonequilibrium phenomena of which practically nothing is known in the dense-gas case.

Goncharov and Levitov[142] investigated the corona discharge in cryogenic helium. In this discharge, the electrode gap usually contains an extended comparatively homogeneous region ("corona trail") in which thermalized charges drift in the external field. It is most accessible for inspection. The mobilities of positive and negative charges have been estimated on the basis of the recorded volt-ampere characteristics. The electron mobility was found to be very low in liquid helium, corresponding to that of electron bubbles, while in supercritical helium the mobility changed abruptly from that of free electrons to that of bubbles as the temperature or pressure was varied. Both the absolute mobility values and the critical density values at which the sharp change in mobility occurred agreed well with the corresponding values obtained from time-of-flight measurements and discussed in Chap. 2, Sec. a). This indicates an important role for trapped electron states in cryogenic discharges in helium.

In very strong fields, the electrons are heated by the field and the system becomes nonequilibrium. The situation is simplified to a degree if heating of the electrons also results in disruption of the localized states. The average energy level $\bar{\varepsilon}$ in the field F can be estimated from the electron-energy balance. Equating the Joulean heat to the losses in elastic collisions with atoms and regarding the cross section q for scattering of an electron on an atom as independent of energy and the electron energy itself as large compared to the temperature of the gas, we obtain a simple expression for $\bar{\varepsilon}$:

$$\bar{\varepsilon} \approx \sqrt{\frac{M}{m}} eFl, \quad l = (Nq)^{-1}.$$

If the free electrons are heated to energies $\bar{\varepsilon} \gg T$, the energy gain upon transition to the bound bubble state is no longer equal to NV (estimate according to the maximum). Going over to the bound state, a hot electron must lose an energy $\bar{\varepsilon}$, and if the latter is larger than $N\bar{V}$, there is no energy advantage at all. Consequently, if $\bar{\varepsilon} > N\bar{V}$, the existence of bubbles is found to be unfavorable. Let us estimate this level F_1, equating $\bar{\varepsilon} = N\bar{V}$. We obtain

$$F_1 \approx 8\pi^2 e N^2 L^3 a_0 \sqrt{\frac{m}{M}}.$$

$F_1 \approx 60$ V/cm under conditions corresponding to the beginning of localization in helium at $T = 4.2$ K.

High field values arise in the puncture of dielectric media. The dependence of the breakdown voltage in helium on temperature and pressure was investigated in Ref. 142. Figure 24 shows the temperature dependence of the sparkover voltage U_{so} of negative polarity at a pressure of 6 atm with its conspicuous maximum. In the neighborhood of this peak, the value of the puncture voltage increases by a large factor, but it still remains much smaller than in the homogeneous-field case.[141] The reason for the appearance of the peak remains unclear. It is no doubt related to features of ionization and recombination kinetics in dense matter that are still poorly understood.

c) Electrical conductivity of a nonideal weakly ionized plasma

In an equilibrium plasma, electrons appear not as a result of injection, but on thermal ionization. If the degree of ionization is low and the density of the neutral atoms is high, interaction between the charged and neutral particles may radically change certain properties of the matter. An example is a plasma of mercury and alkali-metal vapors at temperatures around 2000 K and densities of the order of 10^{21} cm^{-3}.[10]

The most interesting effects are, first, the increase in electrical conductivity due to the interaction, which

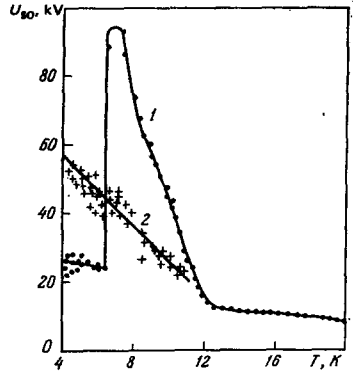

FIG. 24. Sparkover voltage of helium vs. temperature. 1) U_{so}, inhomogeneous field[142] [needle ($R = 0.01$ mm)-plane; electrode gap $d = 9$ mm]; 2) $U_{so}/10$, homogeneous field[141] [sphere ($R = 11$ mm)-plane; equivalent electrode gap $d = 9$ mm]; $p = 6$ atm.

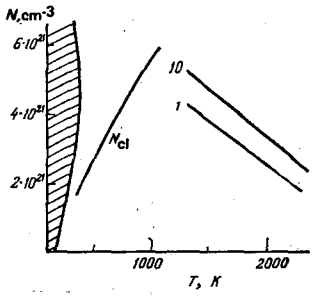

FIG. 25. Density-temperature diagram for Xe. The two-phase region is shaded; the clusterization region is bounded by the N_{cl} curve; curves of equal conductivity are given for $\sigma = 1$ and 10 $\Omega^{-1}\text{cm}^{-1}$ with addition of 2% Cs.

lowers the ionization potential,[143,138,144] and, second, localization of some of the electrons in clusters.[69] Experimental studies of the mercury and alkali plasma at $T \sim 2000$ K are extremely difficult. In our view, a good system for investigation of density effects is dense xenon with a small additive of easily ionized Cs, which yields electrons.

Figure 25 shows a density-temperature diagram for this system. It has been shown that the clusterization region is adjacent to the two-phase xenon region [Chap. 1, Sec. c)]. Theoretical equal-conductivity lines for $\sigma = 1$ and 10 Ω^{-1} cm^{-1} are given for the case in which 2% Cs is added to the xenon. Let us discuss Fig. 25 in greater detail.

We first draw attention to the fact that the conductivity σ does not decrease with increasing N at high densities, as it does in the rarefied plasma, but increases to reach high values. This is because of the large value of ΔE_1—the decrease in the ionization potential; $\beta \Delta E_1 \gg 1$. This quantity is evaluated with a formula similar to (3.3) with other effects also taken into account—the formation of Cs_2^+ and $XeCs^+$ ions and the ground-level shift. The electron concentration

$$n \approx \sqrt{N}\,\lambda_\beta^{-3/2} \exp\left(-\frac{\beta E_I}{2} + \frac{\beta \Delta E_1}{2}\right)$$

increases with N at densities $N \gtrsim 10^{20}$ cm^{-3}, which is what produces the high values of σ. The mobility is determined by (1.1) at high T. The values of σ at smaller T would be of greatest interest. The mobility corrections discussed in Chap. 1, especially the interference correction (1.4), rise sharply in the region next to N_{cl}. Determination of σ becomes very complex in the localization region because it is necessary to have not only the cluster mobility, but also a properly conditioned separation of the electron collective into conduction electrons and electrons that are bound into clusters. Measurements of σ in this region and regions contiguous to it might shed light on these difficult questions, which are general ones in the problem of electron states in dense disordered systems.

[1]E. McDaniel, Collision Phenomena in Ionized Gases, Wiley, 1964.
[2]B. M. Smirnov, Fizika slaboionizovannogo gaza (Physics of the Weakly Ionized Gas), Nauka, Moscow, 1972.
[3]V. I. Gol'danskiĭ, Fizicheskaya khimiya pozitrona i pozitroniya, (The Physical Chemistry of the Positron and Positronium), Nauka, Moscow, 1968.
[4]N. Mott, Electrons in Disordered Structures (Russ. transl.), Mir, Moscow, 1969.
[5]I. M. Lifshitz, Zh. Eksp. Teor. Fiz. **53**, 743 (1967) [Sov. Phys. JETP **26**, 462 (1968)].
[6]M. A. Krivoglaz, Usp. Fiz. Nauk **111**, 617 (1973) [Sov. Phys. Usp. **16**, 856 (1974)].
[8]V. L. Bonch-Bruevich, in: Fizika tverdogo tela (Solid State Physics), VINITI, Moscow, 1965, p. 129 (Itogi nauki).
[9]A. L. Éfros, Usp. Fiz. Nauk **111**, 451 (1973) [Sov. Phys. Usp. **16**, 789 (1974)].
[10]I. T. Yakubov, in: Khimiya plazmy (Plasma Chemistry), No. 1, Atomizdat, Moscow, 1974, p. 120.
[11]B. I. Halperin, M. Lax, Phys. Rev. **148**, 722, 1966.
[12]J. Zittartz, J. S. Langer, *ibid.*, p. 741.
[13]J. Hasted, Physics of Atomic Collisions (Russ. transl.), Mir, Moscow, 1965.
[14]R. Grunberg, Zs. Phys., **204**, 12, 1967.
[15]R. Grunberg, Zs. Naturforsch., **23a**, 12, 1967.
[16]A. Bartels, Phys. Lett. Ser. A **44**, 403 (1973).
[17]H. Lehning, *ibid.*, **29**, 719 (1969).
[18]a) T. F. O'Malley, Phys. Rev. **130**, 1020 (1963). b) K. W. Shwartz, Phys. Rev. Lett., **41**, 239 (1978).
[19]I. T. Yakubov, Zh. Eksp. Teor. Fiz. **57**, 1040 (1969) [Sov. Phys. JETP **30**, 567 (1970)].
[20]J. Lekner, Phys. Rev. **158**, 130 (1957).
[21]L. T. Iakubov, V. I. Roldughin, Phys. Rev. Ser. A **49**, 427 (1974).
[22]J. A. Jahnke, N. A. W. Holzwarth, S. A. Rice, Phys. Rev. Ser. A **5**, 463 (1972).
[23]H. R. Harrison, B. E. Springett, Phys. Lett. Ser. A **35**, 73 (1971).
[24]J. A. Jahnke, M. Silver, Chem. Phys. Lett. **19**, 231 (1973).
[25]A. Bartels, Appl. Phys., **8**, 59 (1975).
[26]J. A. Jahnke, M. Silver, J. P. Hernandez, Phys. Rev. Ser. B **12**, 3420 (1975).
[27]H. R. Harrison, B. E. Springett, Chem. Phys. **10**, 418 (1971).
[28]B. E. Springett, J. Jortner, M. H. Cohen, J. Chem. Phys. **48**, 2720 (1968).
[29]R. A. Ferrell, Phys. Rev. **108**, 167 (1957).
[30]J. B. Smith, J. D. McGervey, A. J. Dahm, *ibid.*, **B 15**, 1378 (1977).
[31]A. Bartels, Phys. Lett. Ser. A **45**, 491 (1973).
[32]L. G. Chistophorou, Intern. J. Rad. Phys. and Chem. (R. L. Platzman memorial issue), **7**, 205 (1975).
[33]B. Huber, Zs. Naturforsch., **24a**, 578 (1969).
[34]V. M. Atrazhev, I. T. Iakubov, J. Phys. Ser. D **10**, 2155 (1977).
[35]V. L. Ginzburg and A. V. Gurevich, Usp. Fiz. Nauk **70**, 201 (1960) [Sov. Phys. Usp. **3**, 115 (1960)].
[36]L. Frommhold, Phys. Rev., **172**, 118 (1968).
[37]L. A. Palkina, B. M. Smirnov, and O. B. Firsov, Zh. Eksp. Teor. Fiz. **61**, 2319 (1972) [Sov. Phys. JETP **34**, 1242 (1972)].
[38]A. Bartels, Phys. Rev. Lett., **28**, 213 (1972).
[39]L. P. Pitaevskiĭ, Zh. Eksp. Teor. Fiz. **37**, 1794 (1959) [Sov. Phys. JETP **10**, 1267 (1960)].
[40]J. Lekner, Phys. Lett. Ser. A **27**, 341 (1968).
[41]M. H. Cohen, J. Lekner, Phys. Rev. **158**, 305 (1967).
[42]N. F. Mott, Adv. Phys., **16**, 49 (1967).
[43]A. G. Khrapak and I. T. Yakubov, Zh. Eksp. Teor. Fiz. **69**, 2042 (1975) [Sov. Phys. JETP **42**, 1036 (1975)].
[44]V. I. Gol'danskiĭ and Yu. S. Sayasov, *ibid.* **47**, 1995 (1964) [**20**, 1339 (1965)].
[45]V. I. Goldanskii, V. P. Shantarovich, Appl. Phys. **3**, 335 (1974).
[46]K. F. Canter, J. O. McNutt, L. O. Roelling, Phys. Rev. Ser. A **12**, 375 (1975).
[47]L. O. Roellig, T. M. Kelly, Phys. Rev. Lett. **18**, 387 (1967).
[48]R. A. Fox, K. F. Canter, M. Fishbein, Phys. Rev. Ser. A **15** A **15**, 1340 (1974).
[49]P. G. Coleman, T. C. Griffith, G. R. Heyland, T. L. Killeen, Phys. Ser. B **8**, 1734 (1975).

[50]P. A. Fraser, Adv. Atom. and Molec. Phys. **4**, 63 (1968).
[51]K. F. Canter, Contemp. Phys. **13**, 457 (1972).
[52]J. D. McNutt, V. B. Summerour, A. D. Ray, and P. H. Huang, H.-J. Chem. Phys. **62**, 1777 (1975).
[53]L. D. Landau, Phys. Zs. Sowjetunion **3**, 664 (1933).
[54]S. I. Pekar, Issledovaniya po elektronnoĭ teorii kristallov (Studies in the Electronic Theory of Crystals), Gostekhizdat, Moscow, 1951.
[55]M. A. Krivoglaz, Fiz. Tverd. Tela (Leningrad) **11**, 2230 (1969) [Sov. Phys. Solid State **11**, 1802 (1970)].
[56]D. A. L. Paul, R. L. Graham, Phys. Rev. **106**, 16 (1957).
[57]J. Wackerle, R. Stump, *ibid.*, p. 18.
[58]R. I. Williams, Can. J. Phys., **35**, 135 (1957).
[59]G. Careri, F. Scaramuzi, Y.O. Thomson, Nuovo Cimento **13**, 186 (1959).
[60]E. Reif, I. Meyer, Phys. Rev. **119**, 1164 (1960).
[61]C. G. Kuper, *ibid.*, **122**, 1007 (1961).
[62]R. G. Arkhipov, Usp. Fiz. Nauk **88**, 185 (1966) [Sov. Phys. Usp. **9**, 174 (1966)].
[63]V. B. Shikin, *ibid.* **121**, 457 (1977) [**20**, 226 (1977)].
[64]K. Hiroike, N. R. Kestner, S. A. Rice, J. Jortner, J. Chem. Phys. **43**, 2625 (1965).
[65]B. E. Springett, M. H. Coben, J. Jorther, Phys. Rev. **159**, 183 (1967).
[66]I. A. Gachechiladze, K. O. Keshishev, and A. I. Shal'nikov, Pis'ma Zh. Eksp. Teor. Fiz. **12**, 231 (1970) [JETP Lett. **12**, 150 (1970)].
[67]V. N. Lebedenko and B. U. Rodionov, *ibid.*, **16**, 583 (1972) [**16**, 411 (1972)].
[68]J. Levine, T. M. Sanders, Phys. Rev. Lett. **8**, 159 (1962).
[69]A. G. Khrapak and N. T. Yakubov, Zh. Eksp. Teor. Fiz. **59**, 945 (1970) [Sov. Phys. JETP **32**, 514 (1971)].
[70]I. T. Iakubov, A. G. Khrapak, Chem. Phys. Lett. **39**, 160 (1970).
[71]L.O. Roellig, T. M. Kelly, Phys. Rev. Lett. **15**, 746 (1965).
[72]K. F. Canter, L. O. Roellig, *ibid.*, **25**, 328 (1970).
[73]A. G. Khrapak and I. T. Yakubov, Pis'ma Zh. Eksp. Teor. Fiz. **23**, 466 (1976) [JETP Lett. **23**, 422 (1976)].
[74]a) P. Hautojarvi, K. Rytsola, P. Tuovinen, A. Vehanen, P Jauho, Phys. Rev. Lett. **38**, 842 (1977). b) M. Manninen, P. Hautojarvi, Phys. Rev. B **17**, 2129 (1978). c) M. J. Stott, E. Zaremba, Phys. Rev. Lett., **38**, 1493 (1977).
[75]H. R. Harrison, T. M. Sanders, B. E. Springett, J. Phys. Ser. B **6**, 908 (1973).
[76]J. Levine, T. M. Sanders, Phys. Rev., **154**, 138 (1967).
[77]V. B. Shikin, Yu. Z. Kovdrya, and A. S. Rybalko, Fiz. Kond. Sost. (Phys.-Tech. Inst. Ukr. Acad. Sci.), **15**, 99 (1971).
[78]A. G. Khrapak and I. T. Yakubov, Teplofiz. Vys. Temp. **11**, 1115 (1973).
[79]K. Huang, Statistical Mechanics, Wiley, 1963.
[80]L. D. Landau and E. M. Lifshitz, Kvantovaya Mekhanika (Quantum Mechanics), Fizmatgiz, Moscow, 1963.
[81]L. S. Kukushkin and V. B. Shikin, Zh. Eksp. Teor. Fiz. **63**, 1830 (1972) [Sov. Phys. JETP **36**, 969 (1973)].
[82]J. P. Hernandez, Phys. Rev. Ser. A **7**, 1755 (1973).
[83]J. P. Hernandez, *ibid.* Ser. B **11**, 1289 (1975).
[84]I. M. Lifshitz, Usp. Fiz. Nauk **83**, 617 (1964) [Sov. Phys. Usp. **7**, 549 (1965)].
[85]I. M. Lifshitz, Zh. Eksp. Teor. Fiz. **57**, 2209 (1969) [Sov. Phys. JETP **30**, 1197 (1970)].
[86]T. P. Eggarter, M. H. Cohen, Phys. Rev. Lett. **25**, 807 (1970).
[87]T. P. Eggarter, M. H. Cohen, *ibid.*, **27**, 129 (1971).
[88]J. P. Hernandez, Phys. Rev. Ser. A **5**, 635 (1972).
[89]T. P. Eggarter, *ibid.*, p. 2496.
[90]J. P. Hernandez, J. M. Ziman, J. Phys. Ser. C **6**, 1251 (1973).
[91]J. A. Northby, T. M. Sanders, Phys. Rev. Lett. **18**, 1184 (1967).
[92]W. B. Fowler, D. L. Dexter, Phys. Rev. **176**, 337 (1968).
[93]B. DuVall, V. Celli, *ibid.*, **180**, 276 (1969).
[94]I. A. Fomin, Pis'ma Zh. Eksp. Teor. Fiz. **6**, 715 (1967) [JETP Lett. **6**, 196 (1967)].
[95]R. A. Young, Phys. Rev. Ser. A **2**, 1983 (1970).
[96]K. W. Shwarz, B. Prasad, Phys. Rev. Lett. **36**, 878 (1976).
[97]W. Legler, Phys. Lett. A **31**, 129 (1970).
[98]M. H. Coopersmith, Phys. Rev. A **4**, 295 (1971).
[99]V. Dallacasa, Phys. Lett. A **57**, 245 (1976).
[100]E. P. Gross, H. Tung-Li, Phys. Rev. **170**, 190 (1968).
[101]V. Celli, M. N. Cohen, M. J. Zuckerman, *ibid.*, **173**, 253.
[102]J. Poitrenaud, E. L. Williams, Phys. Rev. Lett. **29**, 1230 (1972).
[103]J. Howell, M. Silver, Phys. Rev. Lett. **34**, 921 (1975).
[104]Ya. I. Frenkel', Kineticheskaya teoriya zhidkosti (Kinetic Theory of Liquids), Nauka, Leningrad, 1975.
[105]I. T. Iakubov, A. G. Khrapak, Appl. Phys. **16**, 179 (1978).
[106]K. F. Canter, L. O. Roellig, Phys. Rev. A **12**, 386 (1975).
[107]M. Fishbein, K. F. Canter, Phys. Lett. A **55**, 398 (1976).
[108]P. A. Fraser, M. Kraidy, Proc. Phys. Soc. **89**, 533 (1966).
[109]R. J. Drachman, S. K. Houston, J. Phys. Ser. B **3**, 1657 (1970).
[110]J. P. Hernandez, Phys. Rev. A **14**, 1579 (1976).
[111]C. V. Briscoe, S.-I. Choi, A. T. Stewart, Phys. Rev. Lett. **20**, 493 (1968).
[112]P. Smejtek, M. Silver, K. S. Dy, D. G. Onn, J. Chem. Phys. **59**, 1374 (1973).
[113]D. G. Onn, M. Silver, Phys. Rev. A **3**, 1773 (1971).
[114]J. R. Broomall, W. D. Johnson, D. G. Onn, Phys. Rev. B **14**, 2819 (1976).
[115]J. P. Hernandez, M. Silver, Phys. Rev. A **2**, p. 1949 (1970).
[116]T. Miyakawa, D. L. Dexter, *ibid.*, **1**, 513 (1970).
[117]G. Careri, F. Gaeta, Nuovo Cimento **20**, 192 (1961).
[118]W. Lenz, Zs. Phys. **56**, 778 (1929).
[119]A. L. Fetter, in: The Physics of Liquid and Solid Helium, edited by K. H. Benneman, J. B. Ketterson (Wiley, N. Y., 1976).
[120]L. L. Tankersley, J. Low. Temp. Phys., **2**, 451 (1973).
[121]J. Jortner, N. R. Kestner, S. A. Rice, M. H. Cohen, J. Chem. Phys. **43**, 2614 (1965).
[122]W. T. Sommer, Phys. Rev. Lett. **12**, 271 (1964).
[123]a) M. A. Woolf, G. W. Rayfield, *ibid.*, **15**, 235 (1965). b) S. S.-S. Huang, G. R. Freeman, J. Chem. Phys. **68**, 1355 (1978).
[124]E. Hart and M. Angar, The Hydrated Electron, Wiley, 1970.
[125]J. Jortner, M. H. Cohen, Phys. Rev. Ser. B **12**, 1548 (1976).
[126]D. A. Copeland, N. R. Kestner, J. Jortner, J. Chem. Phys. **53**, 1189 (1970).
[127]S. P. Vetchinin and I. T. Yakubov, Teplofiz, Vys. Temp. **15**, 253 (1977).
[128]a) B. D. Michael, E. J. Hart, K. H. Schmidt, J. Phys. Chem., 75, 2798 (1971). b) S. P. Vetchinin, Elektrokhimiya **15**, 421 (1979). c) A. Gaaton, G. Czapski, J. Jortner, J. Chem. Phys. **58**, 2648 (1973).
[129]F. H. Gerter, H. B. Snodgrass, L. Spruch, Phys. Rev. **172**, 110 (1965).
[130]K. R. Atkins, *ibid.*, **116**, 1339 (1959).
[131]S. Hara, P. A. Fraser, J. Phys. B **8**, 219 (1975).
[132]B. H. Bransden, P. K. Hutt, *ibid.*, p. 603.
[133]P. Hautojarvi, K. Rytsola, P. Tuovinen, P. Jauho, in: Conference on Positron Annihilation (Helsing, Denmark, 1976), Paper No. E6.
[134]É. D. Lozanskiĭ and O. B. Firsov, Teoriya iskry (The Theory of the Spark), Atomizdat, Moscow, 1975.
[135]S. E. Derenzo, T. S. Mast, H. Zakland, Phys. Rev. A **9**, 2582 (1974).
[136]V. M. Atrazhev, I. Iakubov, V. I. Roldughin, J. Phys. D **9**, 1735 (1976).
[137]L. T. Kieffer, in: JILA Inform. Center, Rept. No. 13 (University of Colorado, Boulder, 1973).
[138]B. M. Smirnov, Dokl. Akad. Nauk SSSR **195**, 75 (1970) [Sov. Phys. Dokl. **15**, 1050 (1971)].
[139]J. Gerhold, Cryogenics, **12**, 370 (1972).
[140]Issledovaniya vysokovol'tnoĭ izolyatsii pri Kriogennykh

temperaturakh (Studies of High-Voltage Insulation at Cryogenic Temperatures). Collected papers, No. 22, ÉNIN, Moscow, 1975.
[141]A. A. Vinogradov, S. G. Gostev, and V. I. Levitov, *ibid.* p. 18.
[142]V. A. Goncharov and V. I. Levitov, *ibid.* p. 30.
[143]A. A. Vedenov, in: Proceedings of International Conference on Quiscent Plasmas, Frascati, Italy, 1967.
[144]A. G.Khrapak and I. T. Yakubov, Teplofiz. Vys. Temp. 9, 1139 (1971).

Translated by R. W. Bowers